



## Impact of the 2021 La Palma volcanic eruption on air quality: Insights from a multidisciplinary approach



Celia Milford<sup>a</sup>, Carlos Torres<sup>a</sup>, Jon Vilches<sup>b</sup>, Ann-Kathrin Gossman<sup>c</sup>, Frederik Weis<sup>c</sup>, David Suárez-Molina<sup>d</sup>, Omaira E. García<sup>a</sup>, Natalia Prats<sup>a</sup>, África Barreto<sup>a</sup>, Rosa D. García<sup>e,a</sup>, Juan J. Bustos<sup>a</sup>, Carlos L. Marrero<sup>a</sup>, Ramón Ramos<sup>a</sup>, Nayra Chinae<sup>f</sup>, Thomas Boulesteix<sup>g</sup>, Noémie Taquet<sup>g</sup>, Sergio Rodríguez<sup>g</sup>, Jessica López-Darias<sup>h,g</sup>, Michaël Sicard<sup>i,j,k</sup>, Carmen Córdoba-Jabonero<sup>l</sup>, Emilio Cuevas<sup>a,\*</sup>

<sup>a</sup> Izaña Atmospheric Research Center (IARC), State Meteorological Agency of Spain (AEMET), Tenerife, Spain

<sup>b</sup> Department of Ecological Transition, Fight against Climate Change and Territorial Planning, Canary Islands Government, Spain

<sup>c</sup> Palas GmbH, Karlsruhe, Germany

<sup>d</sup> Delegation of AEMET in the Canary Islands (DTCAN), State Meteorological Agency of Spain (AEMET), Spain

<sup>e</sup> TRAGSATEC, Madrid, Spain

<sup>f</sup> Sieltec Canarias, Tenerife, Spain

<sup>g</sup> Department of Life and Earth Sciences, Institute of Natural Products and Agrobiolgy (IPNA-CSIC), San Cristóbal de La Laguna, Spain

<sup>h</sup> Analytical Chemistry Department, La Laguna University, San Cristóbal de La Laguna, Spain

<sup>i</sup> CommSensLab, Universitat Politècnica de Catalunya (UPC), Barcelona, Spain

<sup>j</sup> CTE-CRAE/IEEC, Universitat Politècnica de Catalunya (UPC), Barcelona, Spain

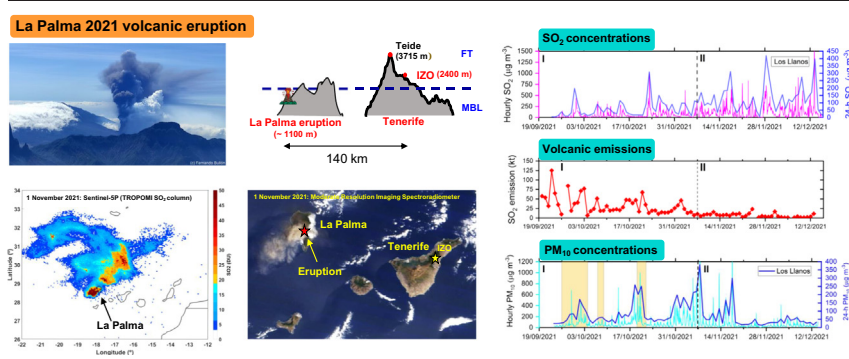
<sup>k</sup> Laboratoire de l'Atmosphère et des Cyclones (LACy), Université de La Réunion, Saint Denis, France

<sup>l</sup> National Institute for Aerospace Technology (INTA), Torrejón de Ardoz, Madrid, Spain

### HIGHLIGHTS

- La Palma 2021 volcanic eruption had a large impact on air quality.
- Ground, satellite and height-resolved measurements provide crucial information.
- SO<sub>2</sub> concentrations at ground-level showed opposite temporal trend to SO<sub>2</sub> emissions.
- Volcanic and desert dust aerosols both impact lower troposphere during the eruption.
- Atmospheric vertical stratification plays key role in eruption impact on air quality.

### GRAPHICAL ABSTRACT



### ARTICLE INFO

Editor: Anastasia Paschalidou

#### Keywords:

Volcanic eruption  
Air quality  
La Palma eruption  
SO<sub>2</sub>  
PM<sub>10</sub> and PM<sub>2.5</sub>  
Volcanic and dust aerosol

### ABSTRACT

The La Palma 2021 volcanic eruption was the first subaerial eruption in a 50-year period in the Canary Islands (Spain), emitting  $\sim 1.8$  Tg of sulphur dioxide (SO<sub>2</sub>) into the troposphere over nearly 3 months (19 September–13 December 2021), exceeding the total anthropogenic SO<sub>2</sub> emitted from the 27 European Union countries in 2019. We conducted a comprehensive evaluation of the impact of the 2021 volcanic eruption on air quality (SO<sub>2</sub>, PM<sub>10</sub> and PM<sub>2.5</sub> concentrations) utilising a multidisciplinary approach, combining ground and satellite-based measurements with height-resolved aerosol and meteorological information. High concentrations of SO<sub>2</sub>, PM<sub>10</sub> and PM<sub>2.5</sub> were observed in La Palma (hourly mean SO<sub>2</sub> up to  $\sim 2600$   $\mu\text{g m}^{-3}$  and also sporadically at  $\sim 140$  km distance on the island of Tenerife ( $> 7700$   $\mu\text{g m}^{-3}$ ) in the free troposphere. PM<sub>10</sub> and PM<sub>2.5</sub> daily mean concentrations in La Palma peaked at

\* Corresponding author at: Izaña Atmospheric Research Center (AEMET), Tenerife, Spain.  
E-mail addresses: [ecuevasa@aemet.es](mailto:ecuevasa@aemet.es) (E. Cuevas), [cmilford2@gmail.com](mailto:cmilford2@gmail.com) (C. Milford).

~380 and 60  $\mu\text{g m}^{-3}$ . Volcanic aerosols and desert dust both impacted the lower troposphere in a similar height range (~0–6 km) during the eruption, providing a unique opportunity to study the combined effect of both natural phenomena. The impact of the 2021 volcanic eruption on  $\text{SO}_2$  and PM concentrations was strongly influenced by the magnitude of the volcanic emissions, the injection height, the vertical stratification of the atmosphere and its seasonal dynamics. Mean daily  $\text{SO}_2$  concentrations increased during the eruption, from 38  $\mu\text{g m}^{-3}$  (Phase I) to 92  $\mu\text{g m}^{-3}$  (Phase II), showing an opposite temporal trend to mean daily  $\text{SO}_2$  emissions, which decreased from 34 kt (Phase I) to 7 kt (Phase II). The results of this study are relevant for emergency preparedness in all international areas at risk of volcanic eruptions; a multidisciplinary approach is key to understand the processes by which volcanic eruptions affect air quality and to mitigate and minimise impacts on the population.

## 1. Introduction

The release of gases and aerosols during volcanic eruptions can have many impacts on the atmosphere, including on air quality, aviation and climate (Langmann et al., 2012; Gettelman et al., 2015; Ilyinskaya et al., 2017) and on the biosphere, for example on terrestrial, marine and freshwater ecosystems (e.g. Caballero et al., 2022; Nogales et al., 2022; Román et al., 2022; Weiser et al., 2022). Volcanic gases mainly include water vapour ( $\text{H}_2\text{O}$ ), carbon dioxide ( $\text{CO}_2$ ), sulphur dioxide ( $\text{SO}_2$ ), hydrogen sulphide ( $\text{H}_2\text{S}$ ), carbon monoxide (CO) and hydrogen halogenides (mainly HCl and HF), some of which are reactive in the atmosphere. Volcanic aerosols include both primary particulate emissions, of different size fractions including ash (defined as particles with diameter < 2 mm) and secondary particulates (e.g. sulphates, metal-bearing aerosols) (Stewart et al., 2021). The impact of volcanic air pollution on human health has recently been reviewed by Stewart et al. (2021) who report studies confirming that exposure to volcanic air pollution can have adverse effects on both respiratory and cardiovascular health as well as other effects such as ocular and dermal irritation.

Air quality and atmospheric impacts of volcanic eruptions have been identified locally (e.g. Searl et al., 2002; Gislason et al., 2015; Andronico and Del Carlo, 2016; Ilyinskaya et al., 2017; Cazorla and Herrera, 2020; Tang et al., 2020; Whitty et al., 2020; Carlsen et al., 2021; Crawford et al., 2021; Trejos et al., 2021) and have also been reported hundreds or thousands of kilometres from the eruption location (e.g. Tu et al., 2004; Newnham et al., 2010; Schäfer et al., 2011; Schmidt et al., 2015; Twigg et al., 2016). For example the April–May 2010 eruption of Eyjafjallajökull volcano, Iceland caused widespread disruption throughout Europe due to volcanic ash in the atmosphere affecting aviation safety (Thomas and Prata, 2011; Langmann et al., 2012). However, despite these studies, there are many locations affected by volcanic eruptions worldwide where air quality measurements are not available (Stewart et al., 2021). It has been estimated that over a billion people live in the proximity of an active volcano (Freire et al., 2019), therefore it is important to understand the air quality impacts of volcanic eruptions.

Numerous studies have identified the adverse effects of air pollution on human health (e.g. WHO, 2013, 2016, 2018; Landrigan et al., 2018; Orellano et al., 2020, 2021), both from natural and anthropogenic sources, and in response, the World Health Organisation (WHO) set Air-Quality Guidelines (AQGs) for particulate matter (PM) ( $\text{PM}_{10}$  and  $\text{PM}_{2.5}$ , PM with aerodynamic diameter < 10  $\mu\text{m}$  and < 2.5  $\mu\text{m}$ , respectively), sulphur dioxide ( $\text{SO}_2$ ), nitrogen dioxide ( $\text{NO}_2$ ), and ozone ( $\text{O}_3$ ). A global update of the WHO AQGs was provided in 2005 (WHO, 2006) and in 2021, new WHO AQGs were published (WHO, 2021) on the basis of evidence that adverse effects of air pollution are observed at lower concentration levels than previously understood. The European Commission (EC) air quality standards for air pollutants in ambient air sets various target and limit values for different pollutants and different averaging times (EC, 2008).

In this study, we examine the air quality impacts of the most recent eruption in the Canary Islands archipelago, which occurred in La Palma between 19 September and 13 December 2021 (lasting 85 days and 8 h) (PEVOLCA, 2021; González, 2022). This was the first subaerial eruption in a 50-year period in the Canary Islands, following the 1971 Teneguia and 1949 San Juan eruptions (also in La Palma). La Palma is the most volcanically active island in the Canary Islands in historical times, hosting six out

of the twelve most recent subaerial eruptions (Hernández-Pacheco and Valls, 1982; Longpré and Felpeto, 2021). Volcanic unrest has been detected at Cumbre Vieja volcano since 2017 (Torres-González et al., 2020), but this unrest accelerated only eight days prior to the eruption (Longpré, 2021). The La Palma 2021 volcanic eruption, located in a zone known as Hoya de Tajogaite, was characterised by extensive lava emissions, (12.4  $\text{km}^2$  lava field), and a very dynamically evolving eruptive style with simultaneous lava fountains (>100 m high), strombolian and/or vulcanian activity, alternating between numerous vents on the eruptive fissure (PEVOLCA, 2021; Castro and Feisel, 2022). The eruption caused considerable destruction and damage to homes, buildings, crops and other infrastructures. La Palma has a population of 83,380 inhabitants (ISTAC, 2021), and a large proportion of the population live in towns and villages on the western side of La Palma close to the 2021 volcanic eruptive centre.

The Canary Islands are located in the sub-tropical eastern North Atlantic, and this region has some distinct features which affect the air quality impacts of the La Palma volcanic eruption, including for example the strong vertical stratification of the lower troposphere (Carrillo et al., 2016; Barreto et al., 2022a). In addition, this region is in the pathway of the long-range transport of mineral dust exported from the Sahara-Sahel region to the North Atlantic, which can expand westward to the Americas (Prospero and Mayol-Bracero, 2013; Tsamalis et al., 2013; Rodríguez et al., 2020; Prospero et al., 2021; Barreto et al., 2022a). This desert dust export from western Africa establishes a dust-laden air layer that is referred to as the Saharan Air Layer (SAL), this dust layer can periodically affect the Canary Islands and increase the particulate load significantly (Viana et al., 2002; Alonso-Pérez et al., 2007; Dominguez-Rodríguez et al., 2020; Rodríguez et al., 2020; Barreto et al., 2022b).

During the 2021 eruption, an unprecedented level of instrumentation and observational capacity were both already in place and deployed as part of the emergency response (ACTRIS, 2021; García et al., 2022; Lopez et al., 2022), involving collaboration among many public organizations and research groups. Observations were obtained from both ground and satellite-based instruments and numerical models using advanced scientific instrumentation and techniques in a manner that was not technically possible in previous subaerial eruptions in the Canary Islands. This level of observational capacity and multidisciplinary approach provides a unique possibility to investigate the 2021 volcanic eruption in La Palma and further develop the understanding of air quality impacts of volcanic eruptions. In this study we evaluate the local and regional impacts of the La Palma 2021 volcanic eruption, concentrating on the air quality impacts of  $\text{SO}_2$  and PM concentrations ( $\text{PM}_{10}$  and  $\text{PM}_{2.5}$ ), as they are considered the most important parameters for population-scale impacts of volcanic air pollution on a longer-term (Stewart et al., 2021).

## 2. Materials and methods

### 2.1. Study area

La Palma in the Canary Islands archipelago is located ~ 445 km west of the African continent in the North Atlantic (Fig. 1a). La Palma is crossed by a north-south volcanic ridge, reaching a maximum height of 2423 m a.s.l. at Roque de los Muchachos. The 2021 volcanic eruption was located on the western slopes of La Palma (Fig. 1c), at a pre-eruption

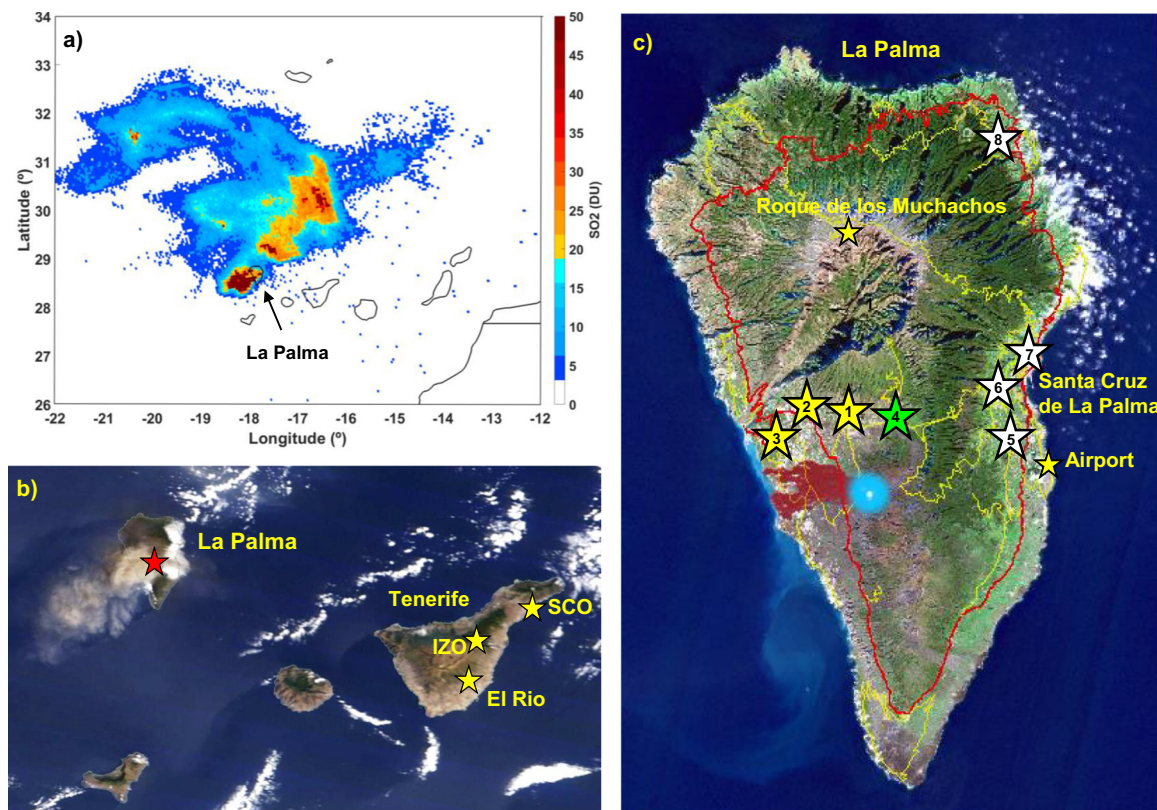


**Fig. 1.** Study site location. a) Satellite column integrated Sulphur Dioxide ( $\text{SO}_2$ ) from Copernicus Sentinel-5P TROPOMI on 1 November 2021 indicating La Palma. b) Image for 1 November 2021 obtained by the Moderate Resolution Imaging Spectroradiometer (MODIS) sensor aboard the Terra satellite showing the western Canary Islands including La Palma and Tenerife, the location of the volcanic eruption is marked with a red star. The location of the Izaña Observatory (IZO), Santa Cruz Observatory (SCO) and the El Rio regional background measurement site are marked with yellow stars. c) Plan view of La Palma indicating the location of the volcanic eruption (blue circle), the lava flow on 17/12/2021 marked in dark red, the air-quality measurement sites, (1) El Paso, (2) Los Llanos de Aridane, (3) Tazacorte, and (4) the AEMET meteorological station (C126A). In addition, the permanent air-quality measurement sites on the eastern side of La Palma are also shown, (5) San Antonio, (6) La Grama, (7) El Pilar and (8) Las Balsas. The red and yellow lines mark roads. Credits: a) Copernicus Sentinel-5P TROPOMI (<https://maps.s5p-pal.com/so2/>), b) We acknowledge the use of imagery provided by services from NASA's Global Imagery Browse Services (GIBS), part of NASA's Earth Observing System Data and Information System and c) Instituto Geográfico Nacional (IGN) (<https://ign-esp.maps.arcgis.com/>).

altitude of  $\sim 900$  m a.s.l. The maximum altitude of the volcanic edifice during the eruption was 1131 m a.s.l. (PEVOLCA, 2021).

The Canary Islands archipelago is generally dominated by the influence of the Azores anticyclone and the quasi-permanent subsidence conditions modulated by the descending branch associated with the Hadley cell. This causes the atmosphere in this region to be characterised by a strong vertical stratification of the lower troposphere, with a strong and stable temperature inversion layer, present for most of the year, with predominance of low-level north-easterly trade winds in the Marine Boundary Layer (MBL) and north-westerly winds above the inversion layer (Carrillo et al., 2016; Azorin-Molina et al., 2018; Barreto et al., 2022a). This predominant atmospheric scenario of background conditions (low aerosol concentration) is interrupted sporadically by desert dust outbreaks (higher aerosol loading) as detailed in the long-term study of aerosol characterization in the sub-tropical eastern North Atlantic (Barreto et al., 2022b).

## 2.2. Air quality measurements

Immediately after the La Palma volcanic eruption began on 19/9/2021, air quality monitoring stations, additional to the existing Canary Islands Air Quality Monitoring Network (AQMN), were deployed by the Canary Islands Government as part of the emergency response, with the collaboration of several public organizations including the Izaña Atmospheric Research Centre (IARC) which is part of the State Meteorological Agency of Spain (AEMET), and the Spanish National Research Council (CSIC).

In this study we analyze air quality data from the following three measurement sites which were deployed to aid the monitoring of the volcanic eruption, located on the western side of La Palma: 1) El Paso and 2) Los Llanos de Aridane (herein denoted as Los Llanos), measurements started on 23/9/2021 (sites operated by Canary Islands Government) and 3) Tazacorte, measurements started on 24/9/2021 (site operated by IARC-AEMET). The population of the three municipal districts of Los Llanos de Aridane, El Paso and Tazacorte, in which these three measurement sites are located, is  $\sim 33,000$  inhabitants (ISTAC, 2021). Details of the location and further details of all the measurement stations utilised in this study are given in Table 1.

The Canary Islands AQMN had four permanent air quality monitoring stations in La Palma, prior to the volcanic eruption. They are all located on the eastern side of La Palma (Fig. 1c), separated from the eruptive centre on the western slope by the Cumbre Vieja volcanic rift which reaches a height of  $\sim 1450$  m a.s.l due east of the eruptive centre. These four sites are: 1) San Antonio, Breña Baja, 2) La Grama, Breña Alta, 3) El Pilar, Santa Cruz de La Palma and 4) Las Balsas, San Andres and Sauces (Table 1).

In addition to the measurement sites in La Palma, we present data from the Izaña Observatory (IZO) in Tenerife and El Rio regional background measurement site, a Canary Islands AQMN site (Fig. 1b). The Izaña Observatory in Tenerife is a high-mountain (2373 m a.s.l.), remote background, permanent observatory located in the free troposphere (FT)  $\sim 140$  km from the eruptive centre, managed by IARC-AEMET. The Izaña Observatory is a World Meteorological Organisation (WMO) Centennial observatory

**Table 1**  
Location and details of measurement sites utilised in this study.

Site name and location	Latitude (° N)	Longitude (° W)	Altitude (m a.s.l.)	Distance from eruptive centre (km)	Site type	Data utilised in this study <sup>a</sup>	Institution
<b>La Palma (west)</b>							
El Paso	28.65	17.88	647	~ 4.4	Temporary <sup>b</sup>	SO <sub>2</sub> , PM <sub>10</sub> , PM <sub>2.5</sub>	CIG AQMN
Los Llanos	28.66	17.91	351	~ 6.2	Temporary <sup>b</sup>	SO <sub>2</sub> , PM <sub>10</sub> , PM <sub>2.5</sub>	CIG AQMN
Tazacorte	28.64	17.93	108	~ 6.9	Temporary <sup>b</sup>	SO <sub>2</sub> , PM <sub>10</sub> , PM <sub>2.5</sub> , lidar profiles	IARC-AEMET
El Paso met station	28.65	17.85	844	~ 4.6	Meteorological station	Wind speed & wind direction at 10 m a.g.l.	AEMET
<b>La Palma (east)</b>							
San Antonio	28.65	17.77	208	~ 10	Suburban background	SO <sub>2</sub> , PM <sub>10</sub> , PM <sub>2.5</sub>	CIG AQMN
La Grama	28.67	17.78	245	~ 11	Suburban industrial	SO <sub>2</sub> , PM <sub>10</sub> , PM <sub>2.5</sub>	CIG AQMN
El Pilar	28.69	17.76	52	~ 13	Urban industrial	SO <sub>2</sub> , PM <sub>10</sub> , PM <sub>2.5</sub>	CIG AQMN
Las Balsas	28.81	17.78	364	~ 23	Rural background	PM <sub>10</sub>	CIG AQMN
<b>Tenerife</b>							
Izaña Observatory	28.31	16.50	2373	~ 140	High-mountain, remote background	SO <sub>2</sub>	IARC-AEMET
Santa Cruz Observatory	28.47	16.24	52	~ 160	Urban background	Lidar profiles	IARC-AEMET
El Río	28.15	16.52	500	~ 140	Regional background	PM <sub>10</sub> , PM <sub>2.5</sub>	CIG AQMN
Güímar station	28.32	16.38	105	~ 150	Radiosonde Station	Radiosonde vertical profiles of pressure, temperature & relative humidity	AEMET

Canary Islands Government (CIG), Air Quality Monitoring Network (AQMN), Izaña Atmospheric Research Centre (IARC), State Meteorological Agency of Spain (AEMET).

<sup>a</sup> Measurement sites have more data available but not employed in this study.

<sup>b</sup> Temporary measurement sites deployed to monitor eruption during emergency response.

which performs high-quality, long-term atmospheric composition measurements (Cuevas et al., 2022).

Measurements of SO<sub>2</sub> concentrations were conducted using ultraviolet (UV) fluorescence analysers at El Paso (Teledyne API T100) and Los Llanos (Teledyne API T100 until 14/12/2021 and Thermo 43i from 14/12/2021 onwards). Measurements of PM<sub>10</sub> and PM<sub>2.5</sub> were conducted at Los Llanos with an Optical Particle Sizer (OPS) (Palas FIDAS 200, Karlsruhe, Germany), an aerosol spectrometer developed specifically for regulatory air pollution control, and in El Paso and Tazacorte, measurements were conducted from 20/11/2021 onwards with an OPS within the air quality instrument (Palas AQ Guard Smart, Germany). The measurements were conducted following European reference methods: EN-14212:2013/AC:2014 for SO<sub>2</sub> and EN-16450:2017 for PM<sub>10</sub> and PM<sub>2.5</sub>. In Tazacorte and Izaña Observatory, SO<sub>2</sub> concentrations were also measured with UV fluorescence analysers, Thermo 43C and Thermo 43C-TL (Trace Level), respectively. During the volcanic eruption, the calibration of the analyser in Tazacorte was verified against the same secondary standard used by the SO<sub>2</sub> analysers of El Paso and Los Llanos. For further details of measurement protocols utilised in Izaña Observatory see González (2012) and Cuevas et al. (2022).

### 2.3. Meteorological parameters: observations and numerical modelling

Ground-based meteorological data was obtained from the El Paso AEMET automatic meteorological station (C126A), which is situated at a distance of 2.7 km from the El Paso air quality station (Fig. 1c). Data included hourly measurements of wind speed and wind direction at 10 m a.g.l., air temperature at 2 m a.g.l. and accumulated precipitation, measurements are conducted following AEMET specifications and WMO guidelines (WMO, 2018).

Radiosonde observational data of vertical profiles of atmospheric pressure, temperature, and relative humidity was obtained from the AEMET automatic radiosonde station in Güímar, Tenerife (Global Climate Observing System, Upper-air Network station 60018). The radiosondes (Vaisala, RS41, Finland) are launched daily at 00:00 and 12:00 UTC, we used the values at 12:00 UTC in this study. The trade wind inversion (TWI) layer base height was derived from these radiosonde observations following Carrillo et al. (2016).

Daily vertical profiles of wind speed and direction have been retrieved from the AEMET numerical weather prediction (NWP) model HARMONIE-AROME (Hirlam Aladin Regional/Meso-scale Operational

NWP in Euromed) Version 43 h2.1.1 (Bengtsson et al., 2017). The spatial resolution of the model is 2.5 × 2.5 km<sup>2</sup>, with 65 vertical levels and a temporal output of 3 h and forecasts until 72 h. The forecast sounding of the grid point closest to the eruptive centre has been used.

As an additional tool, forward trajectories were computed with the FLEXible TRAjectories model (FLEXTRA) (Stohl et al., 1995; Stohl and Seibert, 1998) using ERA5 reanalysis from the European Centre for Medium-Range Weather Forecasts (ECMWF) (Hersbach et al., 2020) obtained through flex extract (v7.1) interface running in gateway mode as an ECMWF member-state user. FLEXTRA input data every 1 h were extracted to a horizontal resolution of 0.28125° × 0.28125°, covering a geographical domain between 18° N to 36° N latitude and 27° W to 0° longitude, with 137 vertical levels. FLEXTRA was configured with the starting point at the eruptive centre with coordinates 28.61° N, 17.87° W, and at pressure levels of 950, 900, 800, 700, 600 and 500 hPa. We obtained a forward trajectory coordinate every 20 min with a 3D wind configuration.

### 2.4. Auxiliary data

#### 2.4.1. Satellite derived volcanic SO<sub>2</sub> emissions

Daily volcanic SO<sub>2</sub> emissions were obtained from the Tropospheric Monitoring Instrument (TROPOMI), onboard the Copernicus Sentinel-5 Precursor (S-5P) platform, which provides complete daily global coverage of key atmospheric air quality and climate components. TROPOMI (launched in October 2017) is a push-broom imaging spectrometer measuring earthshine radiances at eight spectral bands covering from ultraviolet to shortwave infrared wavelengths (Theys et al., 2017), with a high spectral and unprecedented spatial resolution (5.5 × 3.5 km<sup>2</sup> at nadir since August 2019). Here, the daily SO<sub>2</sub> emissions for the 2021 La Palma eruption were obtained from the volcano monitoring platform MOUNTS (Monitoring Unrest from Space; www.mounts-project.com) (for further details of MOUNTS see Valade et al., 2019). MOUNTS downloads the TROPOMI level 2 near-real-time products and converts the vertical column densities of pixels (a 500 × 500 km frame) into SO<sub>2</sub> mass. The daily SO<sub>2</sub> emission corresponds to the sum of the masses of the pixels flagged as SO<sub>2</sub> contaminated (L2-product flag “sulfur dioxide detection flag”, Romahn et al., 2022).

#### 2.4.2. Lidar aerosol vertical distribution observations

A micro-pulse lidar (MPL-4B) was installed on 15/10/2021 in the Tazacorte measurement site as part of the emergency deployment to characterise the volcanic eruption (for further details see ACTRIS, 2021;

Sicard et al., 2022). In addition, the lidar system was used to identify Saharan dust episodes during the volcanic eruption. Lidars are considered the most efficient technique for characterization and continuous monitoring of aerosol vertical distribution, especially if polarization lidar options are available (Ansmann et al., 2012). This technique has been used in previous studies to characterise the evolution of the vertical and seasonal dust distribution in the subtropical North Atlantic region (Berjón et al., 2019; Barreto et al., 2022a). The lidar system in Tazacorte measurement site was used from 15/10/2021 onwards, while before this date, the MPL-4B system operating in Santa Cruz de Tenerife Observatory (SCO) was used. These MPLs are eye-safe elastic lidar operating at 532 nm with depolarization capability, and are the standard lidar system within the global NASA Micro-Pulse Lidar Network (MPLNET, <https://mplnet.gsfc.nasa.gov>) (Welton and Campbell, 2002). See Cuevas et al. (2022) for more details of the lidar system in Santa Cruz de Tenerife.

#### 2.4.3. Tephra deposition measurements

Fresh tephra samples deposited from the eruptive plume were collected in plastic trays covered with paper sheets over measured time intervals. A permanent trap was installed from 20/10/2021 at the IARC-AEMET Tazacorte station, for 24–48 h collection of tephra samples. Additional traps were sporadically set for shorter durations (5–300 min) at different locations in the Aridane Valley between 1 and 8 km from the vents. The sporadic measurements in the Aridane Valley represent “instantaneous” rates, they do not integrate the accumulation of a whole day or several days as in the measurements in Tazacorte station. The tephra samples were stored in air tight plastic bags, later dried (for 24 h at 50 °C) and weighed with a precision balance (Mettler Toledo XS105) in the IZO laboratory.

### 3. Results and discussion

#### 3.1. Air quality surface concentrations

##### 3.1.1. SO<sub>2</sub> concentrations

The temporal evolution of SO<sub>2</sub> surface concentrations measured at the three measurement stations in the Aridane Valley in La Palma are presented for the nearly three months of eruption (19/9/2021–13/12/2021) and for three months post-eruption (14/12/2021–15/03/2022) (Fig. 2a–c), clearly demonstrating that the SO<sub>2</sub> concentrations were strongly impacted by the volcanic eruption, with values well above the typical long-term background values. The measurements also demonstrate that the SO<sub>2</sub> surface concentrations in La Palma generally increased as the volcanic eruption progressed.

During the La Palma volcanic eruption, mean hourly SO<sub>2</sub> surface concentrations at El Paso, Los Llanos and Tazacorte in La Palma were  $40 \pm 126$  (Standard Deviation (SD)),  $95 \pm 133$  and  $56 \pm 103 \mu\text{g m}^{-3}$ , respectively (Fig. 2a–c, Table 2). Maximum hourly mean SO<sub>2</sub> concentrations at El Paso, Los Llanos and Tazacorte were 2593, 1677 and 1623  $\mu\text{g m}^{-3}$ , respectively. SO<sub>2</sub> concentrations exceeded the EC air quality hourly threshold of  $350 \mu\text{g m}^{-3}$  at El Paso, Los Llanos and Tazacorte for a total of 24 h (1.2 % of the eruption period), 82 h (4.0 %) and 37 h (1.8 %), respectively (Table 2). Filonchik et al. (2022) also report SO<sub>2</sub> and PM concentrations during the La Palma 2021 eruption, covering the first month of the eruption (22/9/2021–17/10/2021) and reported that SO<sub>2</sub> hourly concentrations in this first month often exceeded  $400 \mu\text{g m}^{-3}$ .

Mean and median hourly SO<sub>2</sub> concentrations at Izaña Observatory in Tenerife, ~140 km from the volcanic eruptive centre, during the volcanic eruption, were  $33 \pm 296 \mu\text{g m}^{-3}$  and  $0.33 \mu\text{g m}^{-3}$ , respectively (Fig. 2d). SO<sub>2</sub> concentrations at the Izaña Observatory FT background site

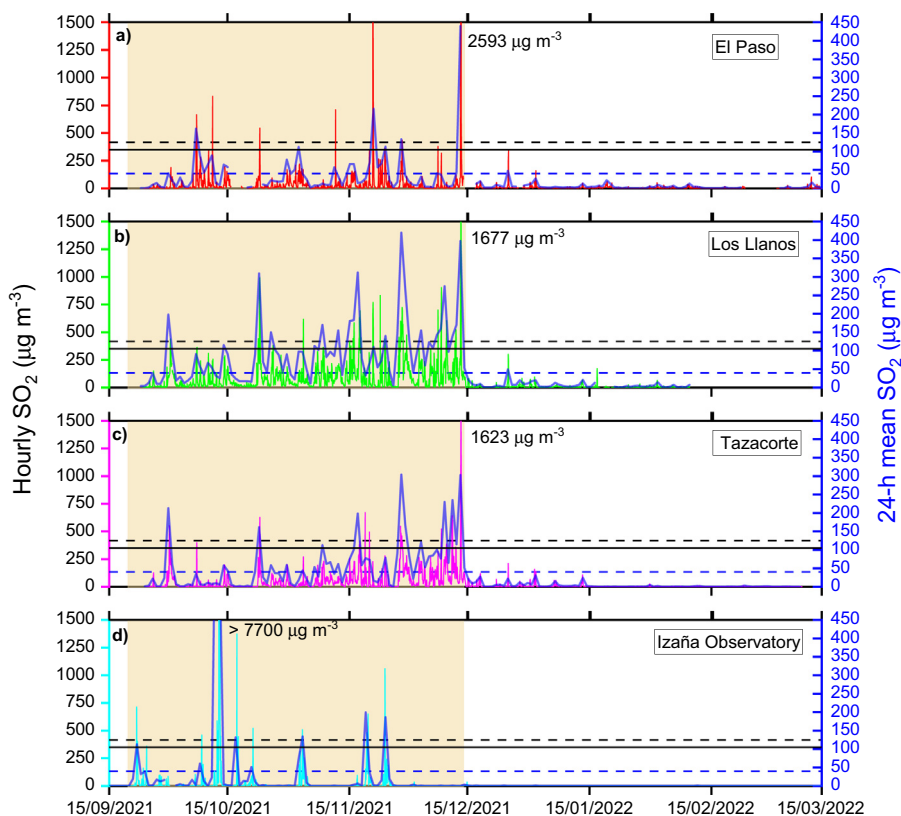


**Fig. 2.** Concentrations of SO<sub>2</sub> at three measurement sites in La Palma: a) El Paso, b) Los Llanos and c) Tazacorte and d) Izaña Observatory, the free troposphere site in Tenerife (15/9/2021–15/3/2022). The left axis indicates hourly mean concentrations and the right axis daily (24-h) mean concentrations. The black horizontal and dashed lines show the European Commission (EC) hourly ( $350 \mu\text{g m}^{-3}$ ) and daily (24-h mean) ( $125 \mu\text{g m}^{-3}$ ) air quality thresholds, respectively. The blue dashed line shows the WHO 2021 24-h mean SO<sub>2</sub> air quality guideline ( $40 \mu\text{g m}^{-3}$ ). The shaded area marks the volcanic eruption period (19/9/2021–13/12/2021).

**Table 2**

Impact of the 2021 volcanic eruption on hourly mean concentrations of SO<sub>2</sub>, PM<sub>10</sub> and PM<sub>2.5</sub> in Aridane Valley (La Palma) measurement stations and Izaña Observatory (IZO) (Tenerife), 19/9/2021–13/12/2021.

Parameter	Mean ( $\mu\text{g m}^{-3}$ )	SD ( $\mu\text{g m}^{-3}$ )	Max ( $\mu\text{g m}^{-3}$ )	Exceedance air quality thresholds and guidelines		
				EC threshold h > 350 $\mu\text{g m}^{-3}$	EC threshold 24-h > 125 $\mu\text{g m}^{-3}$	WHO 2021 guideline 24-h > 40 $\mu\text{g m}^{-3}$
<b>SO<sub>2</sub></b>						
El Paso	40	126	2593	24 (1.2 %)	4 (5 %)	23 (27 %)
Los Llanos	95	133	1677	82 (4.0 %)	20 (24 %)	55 (65 %)
Tazacorte	56	103	1623	37 (1.8 %)	8 (9 %)	38 (45 %)
IZO	33	296	> 7700	28 (1.4 %)	6 (7 %)	10 (12 %)
<b>PM<sub>10</sub></b>						
Los Llanos	77	144	2836	EC threshold 24-h > 50 $\mu\text{g m}^{-3}$ 38 (45 %)	WHO 2021 guideline 24-h > 45 $\mu\text{g m}^{-3}$ 48 (56 %)	
<b>PM<sub>2.5</sub></b>						
Los Llanos	20	22	399		WHO 2005 guideline 24-h > 25 $\mu\text{g m}^{-3}$ 20 (24 %)	WHO 2021 guideline 24-h > 15 $\mu\text{g m}^{-3}$ 44 (52 %)

Measurements started on 23/9/2021 in El Paso and Los Llanos and on 24/9/2021 in Tazacorte, percentages calculated for 85 days of eruption. Standard Deviation (SD).

are normally very low, in the region of 0.2  $\mu\text{g m}^{-3}$  (Cuevas et al., 2022). Maximum hourly mean SO<sub>2</sub> concentrations at IZO exceeded the maximum detection range of the analyser at 7700  $\mu\text{g m}^{-3}$  on 12/10/2021 at 23:00 UTC (the maximum detection range was exceeded for 90 min in total). SO<sub>2</sub> concentrations exceeded the EC hourly threshold of 350  $\mu\text{g m}^{-3}$  in IZO for a total of 28 h (1.4 % of the eruption period).

The impact of the volcanic eruption on SO<sub>2</sub> concentrations at Izaña (> 7700  $\mu\text{g m}^{-3}$  at 140 km distance) is in the range of recorded air quality impacts of the 2014–2015 flood lava eruption at Bárðarbunga (Iceland), one of the largest tropospheric volcanic eruptions worldwide in terms of SO<sub>2</sub> emissions. Total SO<sub>2</sub> emissions over the 6-month Bárðarbunga eruption were estimated between 11 Tg (Gíslason et al., 2015) and 19 Tg (Gauthier et al., 2016). Maximum hourly SO<sub>2</sub> concentrations of 3050  $\mu\text{g m}^{-3}$  at ~80 km distance were reported by Gíslason et al. (2015); 1509  $\mu\text{g m}^{-3}$  at 123 km, 1451  $\mu\text{g m}^{-3}$  at 86 km and 247  $\mu\text{g m}^{-3}$  at 2755 km distance by Schmidt et al. (2015) and 1700  $\mu\text{g m}^{-3}$  at 100 km distance by Ilyinskaya et al. (2017).

With respect to daily (24-h) values, mean SO<sub>2</sub> concentrations during the volcanic eruption period at El Paso, Los Llanos, Tazacorte and IZO were 39 ± 61, 93 ± 85, 55 ± 68 and 33 ± 118  $\mu\text{g m}^{-3}$ , respectively (Table 3). Maximum 24-h mean SO<sub>2</sub> concentrations at El Paso, Los Llanos and Tazacorte were 439, 420 and 304  $\mu\text{g m}^{-3}$ , respectively (Fig. 2a-c). Maximum 24-h mean SO<sub>2</sub> concentrations at IZO exceeded 800  $\mu\text{g m}^{-3}$  (Fig. 2d), an exact maximum 24-h value cannot be given because the SO<sub>2</sub> concentration exceeded the maximum detection range of the analyser. In

comparison, Whitty et al. (2020) reported maximum 24-h mean SO<sub>2</sub> values of 728  $\mu\text{g m}^{-3}$  at a distance of 100 km during the May–August 2018 eruption of Kilauea Volcano, Hawaii.

SO<sub>2</sub> concentrations exceeded the EC 24-h mean air quality threshold of 125  $\mu\text{g m}^{-3}$  at El Paso, Los Llanos and Tazacorte for a total of 4 days (5 % of days of the eruption period), 20 days (24 %) and 8 days (9 %), respectively. In IZO the EC threshold was exceeded for a total of 6 days (7 % of days of the eruption period). It is striking that the maximum hourly mean SO<sub>2</sub> concentration recorded at IZO, in Tenerife, on 12/10/2021 at 23:00 UTC (> 7700  $\mu\text{g m}^{-3}$ ) was three times higher than the maximum hourly mean SO<sub>2</sub> concentration recorded in the three measurement stations in the Aridane Valley in La Palma (2593  $\mu\text{g m}^{-3}$ ) and the maximum 24-h mean SO<sub>2</sub> at IZO also surpassed the La Palma values. This is due to the nearly unperturbed volcanic plume being transported in the similar height range as Izaña Observatory in Tenerife (~ 3 km a.s.l.) and therefore directly impacting the troposphere and the observatory at this altitude, particularly in the first phase of the eruption. In contrast, the measurement stations in the Aridane Valley in La Palma that we utilise in this study were not typically impacted directly by the volcanic plume, as they are located at altitudes lower than the volcanic eruptive centre and are also not downwind of the predominant wind direction during the 2021 eruption (see Section 3.3.4 for more details).

SO<sub>2</sub> concentrations exceeded the more stringent WHO 2021 24-h mean AQG of 40  $\mu\text{g m}^{-3}$  at El Paso for 23 days (27 % of eruption period), at Los Llanos for 55 days (65 %), in Tazacorte for 38 days (45 %) and in IZO for

**Table 3**

Impact of the 2021 volcanic eruption on 24-h mean concentrations of SO<sub>2</sub>, PM<sub>10</sub> and PM<sub>2.5</sub> in Aridane Valley (La Palma) measurement stations and Izaña Observatory (IZO) (Tenerife), 19/9/2021–13/12/2021.

Parameter	Background <sup>a</sup>		Eruption		Volcanic enhancement	
	Mean ± SD ( $\mu\text{g m}^{-3}$ )	Max ( $\mu\text{g m}^{-3}$ )	Mean ± SD ( $\mu\text{g m}^{-3}$ )	Max ( $\mu\text{g m}^{-3}$ )	Mean ± SD ( $\mu\text{g m}^{-3}$ )	Max ( $\mu\text{g m}^{-3}$ )
SO <sub>2</sub> (El Paso)	2.7 ± 3.5	16	39 ± 61	439	36 ± 61	436
SO <sub>2</sub> (Los Llanos)	4.2 ± 4.4	14	93 ± 85	420	89 ± 85	416
SO <sub>2</sub> (Tazacorte)	0.6 ± 0.7	3.0	56 ± 68	304	55 ± 68	304
SO <sub>2</sub> (IZO)	0.23 ± 0.04	0.3	33 ± 118	> 800	32 ± 117	> 800
PM <sub>10</sub> (Los Llanos)	16 ± 12	72	76 ± 72	382	61 ± 70	367
PM <sub>2.5</sub> Los Llanos	7 ± 4	22	20 ± 13	58	14 ± 11	52

<sup>a</sup> Background data for SO<sub>2</sub>: El Paso and Tazacorte, 15/02–15/03/2022 (post-eruption), for Los Llanos, 1–8/2/2022 as measurements end on this date and for IZO, 1–18/9/2021 (pre-eruption). Background (non-volcanic) concentrations of PM<sub>10</sub> and PM<sub>2.5</sub> taken from San Antonio measurement site during eruption, 19/9/2021–13/12/2021. Standard Deviation (SD).

10 days (12 %). Here we note there were more days of the WHO SO<sub>2</sub> AQG exceeded in all three measurement sites of La Palma than in IZO. Although the maximum peak SO<sub>2</sub> concentration in IZO (Tenerife) was larger, the duration and frequency of peak values at IZO were less compared to in La Palma (see Fig. 2), which explains the greater exceedance of the WHO SO<sub>2</sub> AQG values in La Palma. Furthermore, we observe that the last major peak of SO<sub>2</sub> recorded at IZO during the eruption period, was on 24/11/2021 (24-h mean: 187  $\mu\text{g m}^{-3}$ ) (Fig. 2d). After this date, in the latter 18 days of the volcanic eruption, there were only a few, much smaller, briefer spikes in SO<sub>2</sub> concentration registered at IZO. However, in this latter period of the volcanic eruption in La Palma we observe how the SO<sub>2</sub> 24-h mean concentrations, particularly in Los Llanos and Tazacorte, show a trend of increasing concentrations with persistent elevated values (largely >40  $\mu\text{g m}^{-3}$ ) (Fig. 2b and c). In summary, the SO<sub>2</sub> concentration data, both near to the eruptive centre in La Palma, and further away in the free troposphere in Tenerife, highlight the strong impact of the La Palma 2021 volcanic eruption and its effect on SO<sub>2</sub> ambient concentrations.

### 3.1.2. PM surface concentrations

The temporal evolution of PM<sub>10</sub> and PM<sub>2.5</sub> surface concentrations measured in the Aridane Valley in La Palma during the volcanic eruption (19/9/2021–13/12/2021) is presented in Fig. 3a and b, demonstrating the high variability in PM concentrations and the high hourly and daily maximums that were reached. Of the three sites set up to monitor the volcanic eruption in the Aridane Valley, on the western side of La Palma, measurements of PM<sub>10</sub> and PM<sub>2.5</sub> were only conducted for the whole eruption period at the Los Llanos measurement site. During the volcanic eruption period, mean hourly PM<sub>10</sub> and PM<sub>2.5</sub> concentrations at Los Llanos were  $77 \pm 144$  and  $20 \pm 22$   $\mu\text{g m}^{-3}$ , respectively (Table 2). Maximum hourly mean PM<sub>10</sub> and PM<sub>2.5</sub> concentrations at Los Llanos were 2836 and 399  $\mu\text{g m}^{-3}$ , respectively. Regarding daily values, mean 24-h PM<sub>10</sub> and PM<sub>2.5</sub> concentrations during the volcanic eruption period at Los Llanos were  $76 \pm 72$   $\mu\text{g m}^{-3}$  and  $20 \pm 13$   $\mu\text{g m}^{-3}$ , respectively (Table 3). Maximum 24-h mean PM<sub>10</sub> and PM<sub>2.5</sub> concentrations at Los Llanos were 382  $\mu\text{g m}^{-3}$  (Fig. 3a) and 58  $\mu\text{g m}^{-3}$  (Fig. 3b), respectively. For comparison, Whitty et al. (2020) reported maximum 24-h mean PM<sub>2.5</sub> values of 59  $\mu\text{g m}^{-3}$  at a distance of 106 km during the May–August 2018 eruption of Kilauea Volcano, Hawaii. PM<sub>10</sub> concentrations at Los Llanos exceeded the EC 24-h mean air quality threshold (50  $\mu\text{g m}^{-3}$ ) for 38 days (45 % of eruption period) and the WHO 2021 24-h mean PM<sub>10</sub> AQG (45  $\mu\text{g m}^{-3}$ ) for 48 days (56 %) (Fig. 3a). PM<sub>2.5</sub> concentrations at Los Llanos exceeded the WHO 24-h mean PM<sub>2.5</sub> 2005 AQG (25  $\mu\text{g m}^{-3}$ ) and 2021 AQG

(15  $\mu\text{g m}^{-3}$ ) for 20 days (24 % of eruption period) and 44 days (52 %), respectively (Table 2).

It is important to highlight that in the case of SO<sub>2</sub>, the dominant source of SO<sub>2</sub> emission in the study period in La Palma was the volcanic eruption. However, this is not the case for PM<sub>10</sub> and PM<sub>2.5</sub> concentrations, which were a net result of all contributing PM sources during the eruption. There were multiple sources of PM emissions in La Palma during the eruption: there were substantial primary PM emissions (ash particles among the tephra emitted); other PM emissions which arose indirectly from the volcanic eruption, from e.g. fires as the lava advanced on buildings, banana plantations and other vegetation; the formation of secondary particulates (e.g. sulphates), resuspension of volcanic PM and other aerosols produced when the lava flow came into contact with the ocean. In addition to volcanic PM, there were other anthropogenic sources of PM in La Palma such as on-road traffic emissions and there was also the contribution of mineral dust during Saharan air mass episodes.

Lidar vertical profiles at SCO, back trajectory information and reanalysis data were utilised to identify the Saharan air mass episodes that occurred during the volcanic eruption period, in order to examine the contribution of mineral Saharan dust to the PM concentrations. Three Saharan air mass episodes (covering 13 days in total) affecting La Palma during the 85 days of the volcanic eruption, were identified (see Fig. 3 and Fig. S1). The SAL episodes occurred during the following dates: 1) 26/9–3/10/2021, 2) 7–8/10/2021 and 3) 19–21/10/2021. These dust events have been observed to be clearly confined between ~ 1–7 km a.s.l. during the first episode and up to 4 km a.s.l. during the following two episodes, in agreement with the expected seasonal evolution of the SAL vertical extension shown by Barreto et al. (2022a). Median lidar ratio (one-layer method) ranged between 26 and 61 sr, in agreement with results published by Berjón et al. (2019). Polarization measurements provide an important piece of information to characterise the shape of the backscattering particles, ranging from near-zero Volume Depolarization Ratio (VDR) values in the case of spherical particles to the highest VDR values found for non-spherical particles (Ansmann et al., 2012), and consequently provide useful information about the aerosol type. Typical values for VDR and Particle Depolarization Ratio (PDR) for desert dust are given by Freudenthaler et al. (2009) and Ansmann et al. (2012), and references therein. We therefore expect VDR values for desert dust close to 0.20 with PDR values ranging between 0.30 and 0.35. However, higher PDR values are expected for volcanic ash by these authors (0.34), based on 2–3 day transported volcanic plumes, and importantly, lower PDR (0.02) for fine-mode aerosols (such as those sulphates originating from volcanic SO<sub>2</sub> emissions). Fresh volcanic aerosols could present lower PDR values due to a balanced mixing stage

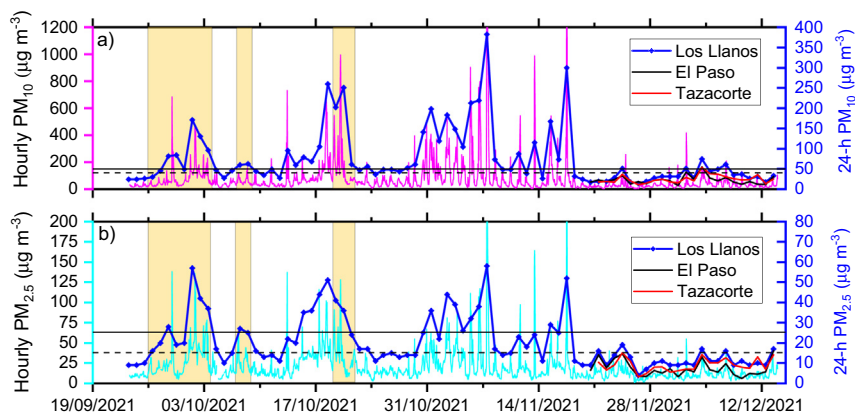


**Fig. 3.** Concentrations of a) PM<sub>10</sub> and b) PM<sub>2.5</sub> at Los Llanos, El Paso and Tazacorte, 19/9/2021–13/12/2021. The left axis indicates hourly mean concentrations and the right axis daily (24-h) mean concentrations. Measurements in El Paso and Tazacorte were only available from 20/11/2021 onwards. The black horizontal and dashed lines in the top panel show the European Commission (EC) 24-h mean PM<sub>10</sub> air quality threshold (50  $\mu\text{g m}^{-3}$ ) and the WHO 2021 24-h mean PM<sub>10</sub> air quality guideline (45  $\mu\text{g m}^{-3}$ ), respectively. The black horizontal and dashed lines in the lower panel show the WHO 2005 24-h mean PM<sub>2.5</sub> (25  $\mu\text{g m}^{-3}$ ) and 2021 (15  $\mu\text{g m}^{-3}$ ) air quality guidelines, respectively. The shaded areas mark the Saharan Air Layer episodes affecting La Palma during the eruption period.

between coarse and fine volcanic particles. Indeed, lidar measurements carried out close to the Mount Etna volcano reported a wide range of PDR values (0.16–0.45) (Pisani et al., 2012; Scollo et al., 2012). This is the case of the PDR mean maximum daily values of  $0.26 \pm 0.08$  obtained during the La Palma volcanic eruption by Córdoba-Jabonero et al. (2023). We observe how the three SAL air mass episodes in September and October 2021 coincide with increasing PM surface concentrations (Fig. 3). However, the maximum PM concentrations observed during the volcanic eruption in November 2021 did not coincide with a SAL episode, therefore these high PM concentrations are attributed to volcanic aerosols.

### 3.2. Volcanic enhancement of surface SO<sub>2</sub> and PM concentrations

In this section, we estimate the volcanic “enhancement” or increment in surface concentrations attributed to the volcanic eruption, in order to further quantify the impact of the La Palma volcanic eruption on air quality levels.

#### 3.2.1. SO<sub>2</sub> concentrations

On the eastern side of La Palma, there were SO<sub>2</sub> measurements prior to the eruption at the permanent air quality monitoring stations in the Canary Islands Air Quality Monitoring Network, therefore to give some context on the volcanic enhancement we examined the SO<sub>2</sub> concentrations in the pre-eruption period. Annual mean SO<sub>2</sub> concentrations at two of the permanent air quality monitoring stations, San Antonio and El Pilar, prior to the volcanic eruption, ranged between 3 and 5  $\mu\text{g m}^{-3}$  in 2019–2020 (CIG, 2020, 2021). There were no exceedances of the EC hourly or daily SO<sub>2</sub> limit values at the permanent air quality monitoring stations in La Palma in the years prior to the 2021 volcanic eruption.

The volcanic enhancement of surface SO<sub>2</sub> concentrations ( $\Delta\text{SO}_2$ ) during the eruption was estimated by subtracting the background concentrations for each measurement site. The mean background SO<sub>2</sub> concentration of the post eruption period in La Palma (mid-February–mid March 2022) was subtracted from the daily (24-h) mean SO<sub>2</sub> concentrations during the volcanic eruption to obtain the daily values of  $\Delta\text{SO}_2$  (Table 3). We utilised the post-eruption period of mid-February–mid March 2022 as in the preceding two months (mid December 2021–mid February 2022), although the volcanic eruption had ceased, there was still some degassing from the volcanic vents which was detected by the La Palma measurement sites as elevated SO<sub>2</sub> concentrations (see Fig. 2a–c).

As expected, we observe a strong volcanic enhancement on both mean and maximum SO<sub>2</sub> concentrations measured during the volcanic eruption. The background SO<sub>2</sub> concentrations are low, at the three measurement stations in the Aridane Valley in La Palma, ranging between 0.6 and 4.2  $\mu\text{g m}^{-3}$  (Table 3) and confirm that there is very little contribution from local sources of SO<sub>2</sub> (which include a power plant and the Santa Cruz de La Palma harbour on the eastern side of La Palma). The dominant source of SO<sub>2</sub> emission in the study period in La Palma was the volcanic eruption, the volcanic SO<sub>2</sub> emissions dominate any small contribution from SO<sub>2</sub> anthropogenic emissions. Values of  $\Delta\text{SO}_2$  (volcanic enhancement of SO<sub>2</sub>) as a mean 24-h value in La Palma range between 36  $\mu\text{g m}^{-3}$  in El Paso to 89  $\mu\text{g m}^{-3}$  in Los Llanos (Table 3). The mean  $\Delta\text{SO}_2$  concentrations are up to 93 times larger compared to background concentrations in La Palma and maximum  $\Delta\text{SO}_2$  24-h concentrations also increase by up to 2 orders of magnitude (e.g. in Tazacorte the maximum background concentration is 3  $\mu\text{g m}^{-3}$  compared to maximum  $\Delta\text{SO}_2$  of 304  $\mu\text{g m}^{-3}$ , Table 3). In Izaña Observatory, where background SO<sub>2</sub> concentrations are very low ( $0.23 \pm 0.04 \mu\text{g m}^{-3}$ , Table 3), representative of the free troposphere and far from the influence of anthropogenic sources, the volcanic enhancement is even greater, with the mean  $\Delta\text{SO}_2$  (32  $\mu\text{g m}^{-3}$ ) and maximum  $\Delta\text{SO}_2$  (> 800  $\mu\text{g m}^{-3}$ ) concentrations being >2 and 3 orders of magnitude greater than the background concentrations, respectively.

#### 3.2.2. PM concentrations

Estimating the volcanic enhancement of surface SO<sub>2</sub> concentrations during the La Palma volcanic eruption is quite straightforward as atmospheric

background concentrations of SO<sub>2</sub> are low in this region. Particulate matter in this subtropical eastern North Atlantic region, however, has a larger atmospheric background and demonstrates high variability and therefore the volcanic enhancement needs to be discriminated from this variable background concentration. This challenge for PM is similar to the challenge in deriving volcanic enhancements for CO<sub>2</sub> as described in Butz et al. (2017). In this region, concentrations of PM<sub>10</sub> and PM<sub>2.5</sub> in the absence of Saharan dust events, are usually low, with typical 24-h mean values of  $\sim 20$  and  $\sim 10 \mu\text{g m}^{-3}$ , respectively (Dominguez-Rodriguez et al., 2020), but concentrations of PM<sub>10</sub> and PM<sub>2.5</sub> increase from tens to hundreds ( $\mu\text{g m}^{-3}$ ) during Saharan dust outbreaks, depending on the severity of the outbreak (see Fig. S2).

To take account of this variability in the PM background, we utilised the PM<sub>10</sub> and PM<sub>2.5</sub> concentrations at the San Antonio suburban background measurement site on the eastern side of La Palma as representative of the daily background or “non-volcanic” concentrations. These non-volcanic concentrations include other contributing PM sources during the eruption such as any contribution of mineral dust during Saharan air mass episodes.

We obtained the daily net volcanic enhancement ( $\Delta\text{PM}$ ) in PM<sub>10</sub> and PM<sub>2.5</sub> at Los Llanos measurement site, by subtracting the daily background (non-volcanic) concentration at San Antonio from the PM<sub>10</sub> and PM<sub>2.5</sub> concentrations in Los Llanos. Only the enhancement at the Los Llanos station is evaluated because its measurement series covers the entire volcanic eruption and the other stations do not. The choice of San Antonio for the background site provides a conservative estimate of the volcanic eruption enhancement as there were days when the San Antonio measurement site was also affected to some degree by the volcanic eruption. However, on examining the data, there were only four days (20–23/11/2021) when the PM<sub>10</sub> and PM<sub>2.5</sub> concentrations at the San Antonio measurement site were affected to a greater degree by the volcanic eruption than the Los Llanos site.

As an additional check on the representativeness of the background (non-volcanic) concentration, we also utilised the PM<sub>10</sub> and PM<sub>2.5</sub> concentrations at the El Rio regional background measurement site in Tenerife. This measurement site has been used for various studies and characterisations of Saharan air mass episodes in the Canary Islands (Viana et al., 2002; Alonso-Pérez et al., 2007; Milford et al., 2020) and is also the measurement site utilised to quantify the contribution of natural dust to daily PM concentrations during dust episodes in the Canary Islands at a national level (e.g. MITECO, 2021). The PM<sub>10</sub> and PM<sub>2.5</sub> concentrations at San Antonio and El Rio measurement site are very similar (see Fig. S2), confirming the San Antonio concentration series as representative of the background PM variability in this region during the volcanic eruption.

We observe a strong volcanic enhancement on both mean and maximum PM<sub>10</sub> and PM<sub>2.5</sub> concentrations measured during the volcanic eruption (Fig. 4). Background or “non-volcanic” PM<sub>10</sub> and PM<sub>2.5</sub> concentrations in La Palma during the eruption are  $16 \pm 12 \mu\text{g m}^{-3}$  and  $7 \pm 4 \mu\text{g m}^{-3}$ , respectively (Table 3). Values of  $\Delta\text{PM}_{10}$  and  $\Delta\text{PM}_{2.5}$  as a mean 24-h value in La Palma are  $61 \pm 70 \mu\text{g m}^{-3}$  and  $14 \pm 11 \mu\text{g m}^{-3}$ , respectively. The maximum 24-h value of  $\Delta\text{PM}_{10}$  and  $\Delta\text{PM}_{2.5}$  in La Palma are 367  $\mu\text{g m}^{-3}$  and 52  $\mu\text{g m}^{-3}$ , respectively. The mean and maximum  $\Delta\text{PM}_{10}$  are 4 and 5 times the background concentrations, respectively, while the mean and maximum  $\Delta\text{PM}_{2.5}$  concentrations are twice the background concentrations. The volcanic enhancement relative to background concentrations is larger in the PM<sub>10</sub> fraction than the PM<sub>2.5</sub> fraction.

Although the volcanic enhancement in PM<sub>10</sub> and PM<sub>2.5</sub> concentrations is substantial, the enhancement in PM in the subtropical eastern North Atlantic region from Saharan air mass episodes can be larger than the observed volcano enhancement, in terms of PM surface concentrations. This is demonstrated by measurements in January 2022 where there were two very intense Saharan air mass episodes with daily mean (24-h) PM<sub>10</sub> peaking at Los Llanos and San Antonio at 560 and 647  $\mu\text{g m}^{-3}$ , respectively, on 16/1/2022, and at 431 and 472  $\mu\text{g m}^{-3}$ , respectively on 30/1/2022 (Fig. S2). Daily mean (24-h) PM<sub>2.5</sub> peaked at Los Llanos and San Antonio at 142 and 155  $\mu\text{g m}^{-3}$ , respectively, on 16/1/2022, and at 116 and 113  $\mu\text{g m}^{-3}$ , respectively on 30/1/2022. In winter and early



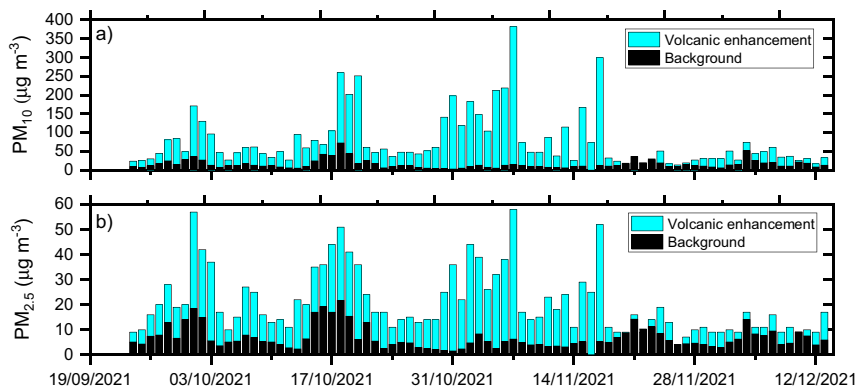


Fig. 4. Daily (24-h mean) volcanic enhancement in Los Llanos and background (non-volcanic) concentrations at San Antonio (La Palma-suburban background) of a)  $PM_{10}$  and b)  $PM_{2.5}$  (19/9/2021–13/12/2021).

spring, the Saharan air mass episodes over the subtropical eastern North Atlantic are usually confined to low altitudes (< 2 km a.s.l.) while in summer, the SAL and dust transport occurs at higher altitudes (~ 1–6 km a.s.l.) (Barreto et al., 2022a,b). The dust episodes in wintertime in this region are more intense in terms of surface PM concentrations than those in summer (Viana et al., 2002); for example, Milford et al. (2020) observed an increment of 84 and 26  $\mu\text{g m}^{-3}$  in  $PM_{10}$  and  $PM_{2.5}$  mean (24-h) concentrations during winter intense dust outbreaks and 35 and 13  $\mu\text{g m}^{-3}$  in summer intense dust outbreaks in this region.

The volcanic PM enhancement was substantial and although the desert dust PM enhancement in the subtropical eastern North Atlantic region can be larger, the duration of the volcanic eruption (85 days), was much longer than the typical Saharan dust episode duration (3–5 days).

### 3.3. Temporal evolution of $SO_2$ and PM concentrations: modulating factors

In this section, we examine the temporal evolution of  $SO_2$  and PM concentrations during the 2021 La Palma volcanic eruption and explore the various factors, both volcanic and atmospheric, that modulate these concentrations. The temporal evolution of various parameters during the eruption period is presented in Fig. 5, these include  $SO_2$  surface concentrations in La Palma (Fig. 5a), daily  $SO_2$  volcanic emissions (according to satellite constrained estimates) (Fig. 5b), measurements of the volcanic eruptive column top height and Trade Wind Inversion (TWI) layer base height (Fig. 5c),  $PM_{10}$  and  $PM_{2.5}$  surface concentrations in La Palma (Fig. 5d), tephra deposition (Fig. 5e) and the  $SO_2/PM_{2.5}$  mass ratio (Fig. 5f).

#### 3.3.1. Volcanic $SO_2$ emissions

The temporal evolution of  $SO_2$  surface concentrations in La Palma during the eruption period demonstrates that the  $SO_2$  concentrations generally increased as the volcanic eruption progressed (Fig. 5a), however, this is in contrast to the temporal trend of the  $SO_2$  volcanic emissions (Fig. 5b). At the start of the volcanic eruption, the daily  $SO_2$  volcanic emissions (according to satellite constrained estimates) were at their greatest, fluctuating in the range ~ 10–85 kt and reaching a maximum of 125 kt on 23/9/2021 (Fig. 5b).

As the eruption progressed, the  $SO_2$  emission rates decreased, with a notable decline from approximately 7/11/2021 onwards. We have denoted this first period of the volcanic eruption with greater  $SO_2$  emission rates, as Phase I. The daily mean and accumulated  $SO_2$  volcanic emission during Phase I were 34 kt and 1.59 Mt., respectively. It is striking to observe the largest peaks in  $SO_2$  surface concentrations in La Palma at the end of the eruption (Fig. 5a, Phase II) when the daily  $SO_2$  emissions were at their lowest; the daily mean and accumulated  $SO_2$  emission during Phase II were 7 kt and 0.25 Mt., respectively. Although Phase I is roughly 55 % of the eruption duration, the total  $SO_2$  mass emitted during Phase I was >6 times larger than in Phase II.

Total  $SO_2$  emitted from the La Palma 2021 volcanic eruption was estimated as ~ 1.84 Tg from satellite constrained estimates (TROPOMI) provided by the MOUNTS volcano monitoring platform (see Section 2.4.1 for more details), this is in agreement with the value provided by PEVOLCA of ~ 2 Tg (PEVOLCA, 2021). Carn et al. (2017) report ~ 23 ± 2 Tg yr<sup>-1</sup> for global passive volcanic  $SO_2$  emissions derived from satellite measurements for 2005–2015, with global eruptive volcanic emissions being more variable and ranging from ~ 0.2 to 10 Tg yr<sup>-1</sup>. Bani et al. (2022) estimate the total volcanic  $SO_2$  flux for Indonesian volcanoes as 1.27–1.69 Tg yr<sup>-1</sup>. Therefore, the La Palma 2021 eruption emitted the equivalent to slightly more than one of the most volcanically active regions of the world.

These values demonstrate the substantial  $SO_2$  emissions of the La Palma 2021 volcanic eruption and their importance on a global scale. Furthermore, the estimate of 1.84 Tg of  $SO_2$  emitted during the nearly 3 months of the La Palma 2021 volcanic eruption exceeds the 1.66 Tg of anthropogenic  $SO_2$  emitted in the 27 countries of the European Union throughout the whole of 2019 (EEA, 2021). The La Palma 2021 volcanic  $SO_2$  emissions are >10 times the total anthropogenic  $SO_2$  emissions reported for 2019 in Spain (0.167 Tg) (MITECO, 2022) and > 100 times the Canary Islands anthropogenic  $SO_2$  emissions (0.016 Tg), evidencing the huge release of  $SO_2$  into the atmosphere from the 2021 eruption and demonstrating how the volcanic emissions dominate the  $SO_2$  anthropogenic emissions in this region.

#### 3.3.2. Meteorological conditions

To explore the factors influencing the surface concentrations, measurements of the Trade Wind Inversion layer base height derived from radiosonde observations (following Carrillo et al., 2016), were utilised to characterise the vertical structure of the atmosphere during the La Palma 2021 volcanic eruption. The TWI height in the Canary Islands region shows a clear seasonal variation, with a minimum value in the summer months and reaching its maximum value in the winter months (Carrillo et al., 2016). The median TWI base height in the Canary Islands region in the summer months is 949 ± 18 m a.s.l. and in the winter months is 1522 ± 21 m a.s.l., with the inversion being thicker and stronger in summer (thickness = 308 ± 36 m a.s.l.,  $\Delta T = 4.6 \pm 0.3$  °C) than in winter (thickness = 210 ± 42 m a.s.l.,  $\Delta T = 2.7 \pm 0.4$  °C) (Carrillo et al., 2016).

During Phase I of the volcanic eruption, the TWI base height was mostly <2000 m (Fig. 5c), with a median value of 1221 m a.s.l., values typical for this season if we compare with the values given in Carrillo et al. (2016). Estimations of the eruptive column top height were obtained from the daily reports issued from the Scientific Committee of the Plan Especial de Protección Civil y Atención de Emergencias por Riesgo Volcánico en la Comunidad Autónoma de Canarias (PEVOLCA) (e.g. PEVOLCA, 2021), indicating that at the start of the eruption, the eruptive column top height reached 6000 m. Therefore, during this initial period of the eruption,

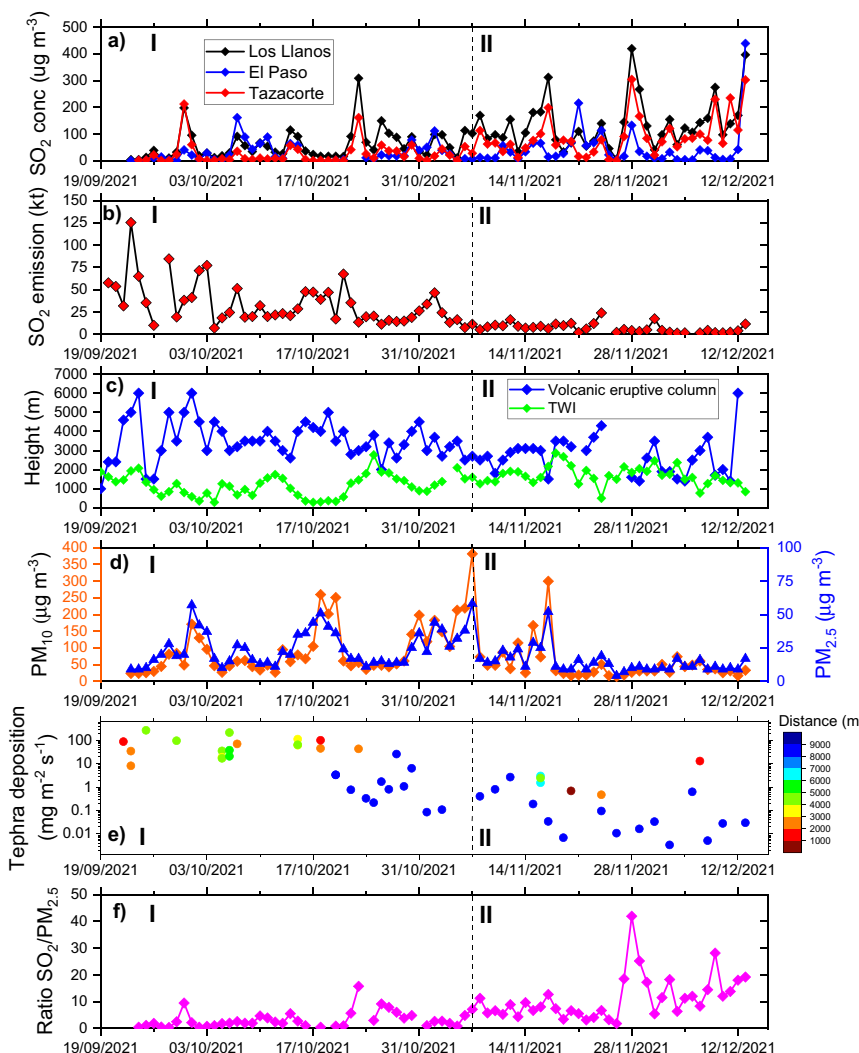


**Fig. 5.** Temporal evolution during La Palma volcanic eruption (19/9/2021–13/12/2021) of a) Daily (24-h mean)  $\text{SO}_2$  concentrations in La Palma, b) Daily  $\text{SO}_2$  volcanic emissions (kt) estimate provided by TROPOMI (credit: ESA, MOUNTS), c) Volcanic eruptive column top height and Trade Wind Inversion (TWI) base height (m a.s.l.). d) Daily (24-h mean)  $\text{PM}_{10}$  and  $\text{PM}_{2.5}$  concentrations in Los Llanos. e) Tephra deposition ( $\text{mg m}^{-2} \text{s}^{-1}$ ) recorded sporadically in various sites in the Aridane Valley and continuously in Tazacorte measurement site (24/10/2021–14/12/2021) (note logarithmic scale on the Y axis) and f)  $\text{SO}_2/\text{PM}_{2.5}$  mass ratio. The vertical dashed line marks the date 7/11/2021 and separates the volcanic eruption into two phases (I and II).

the volcanic  $\text{SO}_2$  emissions were likely injected largely into the free troposphere, above the MBL.

As the volcanic eruption progressed into the months of November and December 2021, the TWI base height increased, to values generally ranging from 1300 to 3000 m (Fig. 5c), with a median value of 1652 m a.s.l., values typical for this season. The volcanic eruptive column height also decreased notably as the eruption progressed and in the latter period of the eruption (Phase II), the eruptive column top height and the TWI base height were often at similar altitudes (Fig. 5c). Consequently, a larger proportion of the  $\text{SO}_2$  emitted by the volcano in the latter stage of the eruption was now likely confined in the MBL rather than being emitted above the MBL into the free troposphere, as in the earlier stage of the eruption. This interplay of the volcanic emissions injection height and prevailing atmospheric conditions determines the impact of volcanic pollutants in the atmosphere, as also concluded by Thomas et al. (2017). These modulating factors lead to the  $\text{SO}_2$  surface concentrations in La Palma increasing as the eruption progressed (as seen in Fig. 5a) rather than decreasing in accordance with the decreasing emission fluxes (as seen in Fig. 5b). As a result of a larger proportion of the volcanic plume (being confined to the MBL in the latter phase of the eruption (Phase II), it is in this phase that we observe the most adverse conditions (maximum hourly  $\text{SO}_2$  concentrations experienced

in La Palma reaching  $\sim 2600 \mu\text{g m}^{-3}$ , well above the typical long-term background values) and largest impacts for  $\text{SO}_2$  surface air quality in La Palma. The majority of the  $\text{SO}_2$  hourly and daily exceedances of air quality thresholds occurred during the MBL dominated Phase II, this is demonstrated in Fig. S3 which shows a time line of exceedances of air quality thresholds during the eruption.

### 3.3.3. Tephra deposition

The temporal evolution of PM concentrations is more complex than that of  $\text{SO}_2$ ; there were multiple sources of PM emissions in La Palma during the eruption. The major source of volcanic PM is the ash plume. The tephra deposition measurements recorded sporadically and instantaneously in various sites in the Aridane Valley and continuously in Tazacorte measurement station (Fig. 5e) present a globally decreasing trend, similar to the trend of daily  $\text{SO}_2$  emissions (Fig. 5b) and to that of the height of the plume (Fig. 5c), reflecting the progressively decreasing pressure in the system (Charco et al., 2022). The tephra deposition rate is generally several orders of magnitude higher during Phase I than during Phase II (Fig. 5e). This is clear from our record at the distal permanent Tazacorte station, although measurements only start on 24/10/2021. This is also apparent for the most proximal measurements, although they can include some intense shorter-term episodes

that are not necessarily maintained over the time scales of the permanent Tazacorte station experiments. The highest ash deposition rate of the deposition measurements presented in this study was  $267 \text{ mg m}^{-2} \text{ s}^{-1}$ , recorded on 25/9/2021 in Phase I, whereas the largest ash deposition recorded in Phase II, in our measurements, was  $13 \text{ mg m}^{-2} \text{ s}^{-1}$  on 16/11/2021. These tephra deposition rates compare with rates of  $6\text{--}700 \text{ mg m}^{-2} \text{ s}^{-1}$  measured during the Eyjafjallajökull eruption (Bonadonna et al., 2011).

### 3.3.4. Volcanic plume transport

The injection height of volcanic gas and aerosol plumes is crucial for both successful forecasting of the plume transport for aviation purposes and for forecasting air quality impacts (Thomas et al., 2017). The subtropical eastern North Atlantic is characterised by a strong vertical stratification of the lower troposphere, which both impedes the vertical growth of the volcanic plume, and results in a typical change of wind direction with height, with a predominance of low-level north-easterly trade winds in the MBL and north-westerly winds above the inversion layer. For these reasons, the height at which the ash and  $\text{SO}_2$  plumes are injected, and the atmospheric layer into which they were emitted, is crucial as this will determine the transport direction of the plumes. The constraint on the vertical growth of the volcanic plume, as well as its confinement in a relatively thin atmospheric layer, with a strong height dependent transport direction, are determining characteristics of the subtropical troposphere that differentiate it from mid latitude and tropical regions, which do not experience such a strong atmospheric vertical stratification.

Wind roses showing the frequency of wind direction during the entire volcanic eruption for both measurements at the surface (10 m a.g.l.) in El Paso meteorological station and for three increasing heights in the atmosphere, at the volcanic eruption location, from the HARMONIE-AROME model at 950 hPa ( $\sim 0.6 \text{ km a.s.l.}$ ), 800 hPa ( $\sim 2 \text{ km a.s.l.}$ ) and 700 hPa ( $\sim 3 \text{ km a.s.l.}$ ) are presented in Fig. 6. Here we observe that measurements at the surface level in El Paso (Fig. 6a) show a dominance of easterly winds while modelled wind direction at  $0.6 \text{ km a.s.l.}$  (Fig. 6b) also show a E-NE dominance, rotating to a dominance of NE winds at  $2 \text{ km a.s.l.}$  (Fig. 6c). The modelled wind direction at 700 hPa, an altitude of  $\sim 3 \text{ km a.s.l.}$ , however, now shows a much wider set of wind directions, with both NE and SW directions as well as NW (Fig. 6d).

The wind rose diagrams demonstrate that in the lower levels of the troposphere during the La Palma 2021 eruption, the dominant wind direction was E-NE, this will have led to any ash and  $\text{SO}_2$  plumes present at these altitudes being transported to the W-SW (that is towards the Aridane Valley and western slopes, see Fig. 1). Any plumes injected at higher levels of the troposphere, e.g. at or above  $3 \text{ km}$ , will have

experienced a greater range of wind directions and been dispersed in various directions including to the NE and SE as well as to the SW.

Three example days illustrating these points are depicted in Fig. 7. The first example day is 12/10/2021, when the maximum  $\text{SO}_2$  concentration was detected at Izaña Observatory. The image (Fig. 7a) clearly shows the plume being transported to the east of La Palma and FLEXTRA forward trajectories indicate SW transport at lower altitudes and easterly transport at higher altitudes (Fig. 7d). This is corroborated by satellite imagery of the  $\text{SO}_2$  plume (Fig. 7g). The second example day is 13/10/2021 (Fig. 7b), where SW transport still dominates at lower altitudes but now the image clearly shows the volcanic plume being split and transported both eastwards and westwards and this is demonstrated by the westward transport of the forward trajectory at 700 hPa ( $\sim 3 \text{ km}$ ) and eastward transport at 600 hPa ( $\sim 4.3 \text{ km}$ ) and above. The third example day is 7/11/2021 (Fig. 7c), the day of maximum PM surface concentrations (see Fig. 5d). The image demonstrates that the volcanic plume height is now reduced and dispersion of the plume into the lower levels of the troposphere can be observed. The forward trajectories for 7/11/2021 show SW-W transport at all altitudes (Fig. 7f), the satellite imagery of the  $\text{SO}_2$  plume corroborates this westerly transport (Fig. 7i).

Volume depolarization ratios from the micro-pulse lidar profiles in SCO and Tazacorte are presented in Fig. 7 for the same three example days, to corroborate the heights of the plumes in the different events and the type of aerosol. The profiles taken at SCO (Fig. 7j and k), show VDR values between 0.05 and 0.20 in a highly stratified volcanic plume, extending between 1.5 and 3 km. The lidar profile of 7/11/2021 in Tazacorte (Fig. 7l) shows slightly higher VDR values (up to 0.22) and also demonstrates that the height of the volcanic aerosol is now clearly lower, extending from the surface up to around 2 km height, and confined within the MBL.

The vertical stratification of the lower troposphere defined the transport of the La Palma 2021 eruption plume and it may well have been dispersed both within and above the MBL at times during the eruption. Any volcanic aerosol confined in the lower levels of the troposphere, according to the predominant W-SW transport at these altitudes, will have affected the Aridane Valley and western slopes of La Palma. These factors and the greater volcanic emission in the first phase of the volcanic eruption likely led to the higher PM concentrations observed in the earlier phase of the eruption. The three Saharan air mass episodes that were identified also occurred during Phase I of the volcanic eruption therefore this additional non-volcanic PM source increased the particulate load during this period.

The interplay of these influencing factors leads to the most adverse conditions (maximum hourly and daily  $\text{PM}_{10}$  and  $\text{PM}_{2.5}$  concentrations)

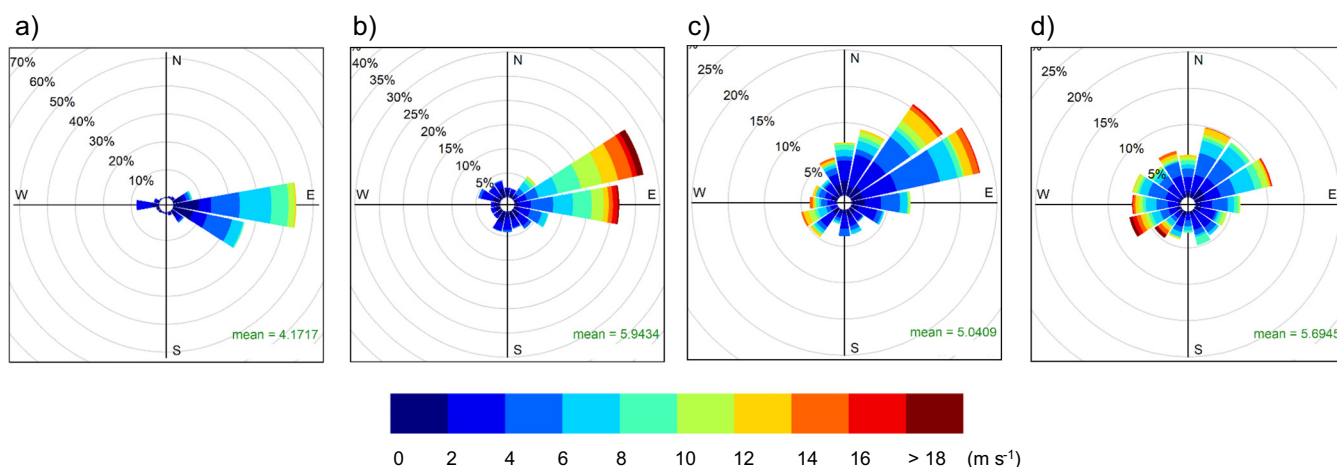
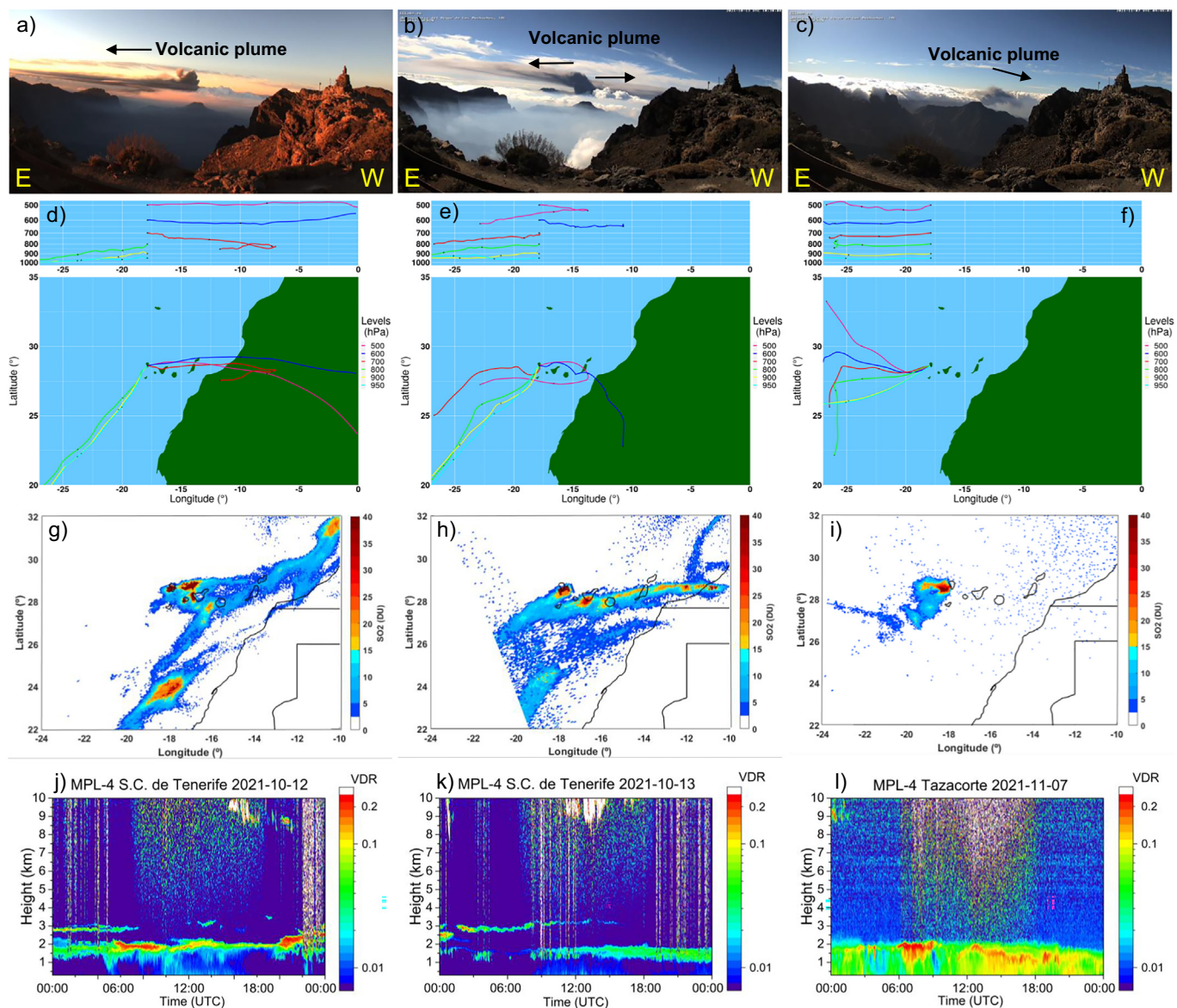


Fig. 6. Wind rose diagrams for a) surface measurements (10 m a.g.l.) El Paso meteorological station and HARMONIE-AROME simulated wind vectors for the volcanic eruption location at b) 950 hPa ( $\sim 0.6 \text{ km a.s.l.}$ ), c) 800 hPa ( $\sim 2 \text{ km a.s.l.}$ ) and d) 700 hPa ( $\sim 3 \text{ km a.s.l.}$ ) for the entire eruption period (19/9/2021–13/12/2021). Graphics were generated with Openair software (Carslaw and Ropkins, 2012).



**Fig. 7.** Images taken from webcam at Roque de los Muchachos facing south for a) 12/10/2021 07:15 UTC, b) 13/10/2021 10:30 UTC and c) 7/11/2021 09:45 UTC. Credit: Proyecto EELabs, IAC (Instituto Astrofísico de Canarias). Note that the East direction is shown on the left of the image and West on the right. d) to f) Forward trajectories (72 h), starting point at the eruptive centre, from FLEXTRA using ERA5 reanalysis at six pressure levels (950, 900, 800, 700, 600 and 500 hPa). g) to i) Satellite column integrated SO<sub>2</sub> from TROPOMI. Credit: Copernicus Sentinel-5P TROPOMI. Micro-pulse lidar volume depolarisation ratio profiles extracted for Santa Cruz, j) (12/10/2021) and k) (13/10/2021) and Tazacorte l) (7/11/2021).

and largest impacts for PM<sub>10</sub> and PM<sub>2.5</sub> surface air quality in La Palma occurring in the earlier part of the La Palma 2021 volcanic eruption (Phase I), in contrast to the largest SO<sub>2</sub> impacts observed in Phase II (see Fig. 5 and Fig. S3). Indeed, the data demonstrates that the majority of the PM<sub>10</sub> and PM<sub>2.5</sub> exceedances of air quality thresholds occurred during Phase I (Fig. S3). This behaviour is also illustrated by the evolution of the SO<sub>2</sub>/PM<sub>2.5</sub> concentration ratio during the volcanic eruption (Fig. 5f), which demonstrates how the PM<sub>2.5</sub> concentrations dominate in Phase I of the eruption while the SO<sub>2</sub> concentrations dominate in Phase II.

It is important for air quality managers or for future studies of the health impacts of the La Palma 2021 volcanic eruption to note that simultaneous exposure of both SO<sub>2</sub> gas and volcanic PM occurred during the eruption, and this should be further studied particularly in terms of public health implications. It is also important to highlight that the temporal evolution of SO<sub>2</sub> gas and volcanic PM showed opposite temporal trends throughout the eruption, leading to a dominance of PM concentrations in Phase I of the eruption and of SO<sub>2</sub> concentrations in Phase II, therefore the chemical

composition of the plume originating from the volcanic eruption likely varied temporally during the La Palma 2021 eruption. Differences in the chemical composition of volcanic plumes and their subsequent health effects have been studied by Carlsen et al. (2021) and various studies have investigated the health effects of both SO<sub>2</sub> gas and sulphate aerosol exposure from volcanic eruptions (e.g. Longo, 2013). Epidemiological studies are currently being implemented to study the health effects of the La Palma 2021 eruption on various population groups (e.g. Ruano-Ravina et al., 2023). Further studies are needed to determine the chemical composition of the atmospheric aerosols and their temporal evolution during the La Palma 2021 volcanic eruption and their impact on health.

#### 4. Conclusions

The La Palma 2021 eruption was the first subaerial eruption after a 50-year quiescence in the Canary Islands and the longest volcanic eruption in La Palma in the last five centuries, causing considerable destruction and

damage to homes, buildings, crops and other infrastructures. This study conducts a comprehensive evaluation of the impact of this eruption on air quality, covers the entire 85 days of the process (19/9–13/12/2021) and employs a multidisciplinary approach, including measurements from instrumentation already in place in La Palma and deployed as part of the emergency response. High concentrations of SO<sub>2</sub>, PM<sub>10</sub> and PM<sub>2.5</sub> were observed at ground level in La Palma (showing a strong volcanic enhancement compared to background concentrations) and also sporadically at ~ 140 km distance on the island of Tenerife, in the free troposphere at Izaña Observatory (~ 2.4 km a.s.l.). An unusual feature of the volcanic eruption was that volcanic aerosols and desert dust both impacted the lower troposphere in a similar height range (~ 0–6 km), therefore the air quality in La Palma during the volcanic eruption was impacted by both natural phenomena concurrently. This led to a greater increase in PM surface concentrations and this cocktail of SO<sub>2</sub> coupled with volcanic and dust aerosol should be further studied particularly in terms of public health implications. The impact of the La Palma 2021 volcanic eruption on surface SO<sub>2</sub> and PM concentrations was strongly influenced by the substantial magnitude of the volcanic emissions (~ 1.8 Tg), the injection height of emissions and the strong vertical stratification of the atmosphere and its seasonal dynamics in this region. As a consequence of the interplay of these modulating factors, SO<sub>2</sub> concentrations at ground-level showed an opposite temporal evolution to particulate matter and increased in the latter phase of the eruption, when a greater proportion of the plume was confined to lower levels of the troposphere, despite significantly reduced SO<sub>2</sub> volcanic emissions in this phase. The results of this study are relevant for emergency preparedness for future volcanic eruptions in the subtropical region and for all international areas at risk of volcanic eruptions; a multidisciplinary approach is key in understanding the processes by which volcanic eruptions affect air quality and to mitigate and minimise impacts on the population.

#### CRedit authorship contribution statement

All authors contributed to the writing of the manuscript and to data curation. C.M., C.T., O. G., N.P., T.B., N.T., S.R. and E.C contributed to conceptualization and formal analysis.

#### Data availability

Data will be made available on request.

#### Declaration of competing interest

The authors declare that they have no known competing financial interests or personal relationships that could have appeared to influence the work reported in this paper.

#### Acknowledgements

The authors gratefully acknowledge the extraordinary effort carried out by the AEMET staff (both in La Palma and in support of the activities in La Palma) during the volcanic eruption, from the Izaña Atmospheric Research Center and the Delegation of AEMET in the Canary Islands. We thank the CSIC deployment service during the eruption and its coordination by Manuel Nogales. We also gratefully acknowledge the dedication and information provided by the PEVOLCA Scientific Committee and all the support received from the insular and local governments (Cabildo Insular de La Palma and the Ayuntamientos de Tazacorte, Los Llanos de Aridane and El Paso). The authors would also like to thank the Canary Islands Government for data from their Air Quality Monitoring Network and the MPL Network (MPLNET) for their support to the lidar measurements used in this paper. The authors also acknowledge the support from ACTRIS and ACTRIS-Spain, the Spanish Ministry of Science and Innovation and the support from the European Union H2020 program through the following projects (PID2019-

104205GB-C21/AEI/10.13039/501100011033, EQC2018-004686-P, PID2019-103886RB-I00/AEI/10.13039/501100011033 and PID2020-521-118793GA-I00) and programs (GA No. 654109, 778349, 871115, 101008004 and 101086690). Research activities of the CSIC staff during the eruption were funded by CSIC through the CSIC-PIE project with ID numbers PIE20223PAL009 and PIE20223PAL013 (Real Decreto 1078/2021, de 7 de diciembre). Part of this study was performed within the framework of the project AERO-EXTREME (PID2021-125669NB-I00) funded by the Spanish State Research Agency (AEI) and ERDF funds.

#### Appendix A. Supplementary data

Supplementary data to this article can be found online at <https://doi.org/10.1016/j.scitotenv.2023.161652>.

#### References

- ACTRIS, 2021. ACTRIS-Spain coordinating unprecedented actions for the Cumbre Vieja volcanic emergency. Available at <https://www.actris.eu/news-events/news/actris-spain-coordinating-unprecedented-actions-cumbre-viejavolcanic-emergency>.
- Alonso-Pérez, S., Cuevas, E., Querol, X., Viana, M., Guerra, J.C., 2007. Impact of the saharan dust outbreaks on the ambient levels of total suspended particles (TSP) in the marine boundary layer (MBL) of the subtropical eastern North Atlantic Ocean. *Atmos. Environ.* 41, 9468–9480. <https://doi.org/10.1016/j.atmosenv.2007.08.049>.
- Andronico, D., Del Carlo, P., 2016. PM10 measurements in urban settlements after lava fountain episodes at mt. Etna, Italy: pilot test to assess volcanic ash hazard to human health. *Nat. Hazards Earth Syst. Sci.* 16, 29–40. <https://doi.org/10.5194/nhess-16-29-2016>.
- Ansmann, A., Seifert, P., Tesche, M., Wandinger, U., 2012. Profiling of fine and coarse particle mass: case studies of saharan dust and Eyjafjallajökull/Grimsvötn volcanic plumes. *Atmos. Chem. Phys.* 12, 9399–9415. <https://doi.org/10.5194/acp-12-9399-2012>.
- Azorin-Molina, C., Menendez, M., McVicar, T.R., Acevedo, A., Vicente-Serrano, S.M., Cuevas, E., Minola, L., Chen, D., 2018. Wind speed variability over the Canary Islands, 1948–2014: focusing on trend differences at the land–ocean interface and below–above the trade-wind inversion layer. *Clim. Dyn.* 50, 4061–4081. <https://doi.org/10.1007/s00382-017-3861-0>.
- Bani, P., Oppenheimer, C., Tsanev, V., Scaillet, B., Primulyana, S., Saing, U.B., Alfianti, H., Marlia, M., 2022. Modest volcanic SO<sub>2</sub> emissions from the Indonesian archipelago. *Nat. Commun.* 13, 3366. <https://doi.org/10.1038/s41467-022-31043-7>.
- Barreto, Cuevas, E., García, R.D., Carrillo, J., Prospero, J.M., Ilić, L., Basart, S., Berjón, A.J., Marrero, C.L., Hernández, Y., Bustos, J.J., Ničković, S., Yela, M., 2022a. Long-term characterisation of the vertical structure of the Saharan Air Layer over the Canary Islands using lidar and radiosonde profiles: implications for radiative and cloud processes over the subtropical Atlantic Ocean. *Atmospheric Chemistry and Physics* 22, 739–763. <https://doi.org/10.5194/acp-22-739-2022>.
- Barreto, A., García, R.D., Guirado-Fuentes, C., Cuevas, E., Almansa, A.F., Milford, C., Toledano, C., Expósito, F.J., Díaz, J.P., León-Luis, S.F., 2022b. Aerosol characterisation in the subtropical eastern North Atlantic region using long-term AERONET measurements. *Atmos. Chem. Phys.* 22, 11105–11124. <https://doi.org/10.5194/acp-22-11105-2022>.
- Bengtsson, L., Andrae, U., Aspeli, T., Batrak, Y., Calvo, J., Gleeson, E., Hansen-Sass, B., Homleid, M., Hortal, M., Ivarsson, K.I., Lenderink, G., Niemelä, S., Nielsen, K.P., Onvlee, J., Rontu, L., Samuelsson, P., Muñoz, D.S., Rooy, W.D., Subias, A., Tijn, S., Toll, V., Yang, X., Koltzow, M., 2017. The HARMONIE-AROME model configuration in the ALADIN-HIRLAM NWP system. *Monthly Weather Review* 145, 1919–1935. <https://doi.org/10.1175/MWR-D-16-0417.1>.
- Berjón, A., Barreto, A., Hernández, Y., Yela, M., Toledano, C., Cuevas, E., 2019. A 10-year characterization of the saharan air layer lidar ratio in the subtropical North Atlantic. *Atmos. Chem. Phys.* 19, 6331–6349. <https://doi.org/10.5194/acp-19-6331-2019>.
- Bonadonna, C., Genco, R., Gouhier, M., Pistolesi, M., Cioni, R., Alfano, F., Hoskuldsson, A., Ripepe, M., 2011. Tephra sedimentation during the 2010 Eyjafjallajökull eruption (Iceland) from deposit, radar, and satellite observations. *J. Geophys. Res. Solid Earth* 116. <https://doi.org/10.1029/2011JB008462>.
- Butz, A., Dinger, A.S., Bobrowski, N., Kostinek, J., Fieber, L., Fischerkeller, C., Giuffrida, G.B., Hase, F., Klappenbach, F., Kuhn, J., Lübcke, P., Tirtzip, L., Tu, Q., 2017. Remote sensing of volcanic CO<sub>2</sub>, HF, HCl, SO<sub>2</sub>, and BrO in the downwind plume of Mt. Etna. *Atmospheric Measurement Techniques* 10, 1–14. <https://doi.org/10.5194/amt-10-1-2017>.
- Caballero, I., Román, A., Tovar-Sánchez, A., Navarro, G., 2022. Water quality monitoring with Sentinel-2 and Landsat-8 satellites during the 2021 volcanic eruption in La Palma (Canary Islands). *Sci. Total Environ.* 822, 153433. <https://doi.org/10.1016/j.scitotenv.2022.153433>.
- Carlsen, H.K., Ilyinskaya, E., Baxter, P.J., Schmidt, A., Thorsteinsson, T., Pfeffer, M.A., Barsotti, S., Dominici, F., Finnbjörnsdóttir, R.G., Jóhannsson, T., Aspelund, T., Gíslason, T., Valdimarsdóttir, U., Briem, H., Gudnason, T., 2021a. Increased respiratory morbidity associated with exposure to a mature volcanic plume from a large Icelandic fissure eruption. *Nat. Commun.* 12, 2161. <https://doi.org/10.1038/s41467-021-22432-5>.
- Carn, S.A., Fioletov, V.E., McLinden, C.A., Li, C., Krotkov, N.A., 2017. A decade of global volcanic SO<sub>2</sub> emissions measured from space. *Sci. Rep.* 7, 44095. <https://doi.org/10.1038/srep44095>.

- Carrillo, J., Guerra, J.C., Cuevas, E., Barrancos, J., 2016. Characterization of the marine boundary layer and the trade-wind inversion over the sub-tropical North Atlantic. *Bound.-Layer Meteorol.* 158, 311–330. <https://doi.org/10.1007/s10546-015-0081-1>.
- Carlslaw, D.C., Ropkins, K., 2012. Openair — an R package for air quality data analysis. *Environ. Model Softw.* 27–28, 52–61. <https://doi.org/10.1016/j.envsoft.2011.09.008>.
- Castro, J.M., Feisel, Y., 2022. Eruption of ultralow-viscosity basanite magma at Cumbre Vieja, La Palma, Canary Islands. *Nature Communications* 13, 3174. <https://doi.org/10.1038/s41467-022-30905-4>.
- Cazorla, M., Herrera, E., 2020. Air quality in the Galapagos Islands: a baseline view from remote sensing and in situ measurements. *Meteorol. Appl.* 27, e1878.
- Charco, M., González, P., García-Cañada, L., del Fresno, C., 2022. Pronosticando el fin de la erupción de La Palma 2021 (Islas Canarias) mediante deformaciones GNSS. *Presentación oral en la sesión S.04. Volcanología. 10 Asamblea Hispano-Portuguesa de Geodesia y Geofísica. 28 Nov- 1 Dec.*
- CIG, 2020. Informe Calidad del aire Canarias 2019. Canary Islands Government. <https://www3.gobiernodecanarias.org/medioambiente/calidaddelaire/documentos.do>.
- CIG, 2021. Informe Calidad del aire Canarias 2020. Canary Islands Government. <https://www3.gobiernodecanarias.org/medioambiente/calidaddelaire/documentos.do>.
- Córdoba-Jabonero, C., Sicard, M., Barreto, A., Toledano, C., López-Cayuela, M., Gil-Díaz, C., García, O., Carvajal-Pérez, C., Comerón, A., Ramos, R., Muñoz-Porcar, C., Rodríguez-Gómez, A., 2023. Fresh volcanic aerosols injected in the atmosphere during the volcano eruptive activity at the cumbre vieja area (La Palma, Canary Islands): temporal evolution and vertical impact. *Atmos. Environ.* (submitted to journal).
- Crawford, B., Hagan, D.H., Grossman, I., Cole, E., Holland, L., Heald, C.L., Kroll, J.H., 2021. Mapping pollution exposure and chemistry during an extreme air quality event (the 2018 Kilauea eruption) using a low-cost sensor network. *Proceedings of the National Academy of Sciences* 118, e2025540118. <https://doi.org/10.1073/pnas.2025540118>.
- Cuevas, E., Milford, C., Barreto, A., Bustos, J.J., García, O.E., García, R.D., Marrero, C., Prats, N., Ramos, R., Redondas, A., Reyes, E., Rivas-Soriano, P.P., Romero-Campos, P.M., Torres, C.J., Schneider, M., Yela, M., Belmonte, J., Almansa, F., López-Solano, C., Basart, S., Werner, E., Rodríguez, S., Afonso, S., Alcántara, A., Alvarez, O., Bayo, C., Berjón, A., Carreño, V., Castro, N.J., China, N., Cruz, A.M., Damas, M., Gómez-Trueba, V., González, Y., Guirado-Fuentes, C., Hernández, C., León-Luís, S.F., López-Fernández, R., López-Solano, J., Parra, F., Pérez de la Puerta, J., Rodríguez-Valido, M., Sálamo, C., Santana, D., Santo-Tomás, F., Sepúlveda, E., Serrano, A., 2022. In: Cuevas, E., Milford, C., Tarasova, O. (Eds.), *Izaña Atmospheric Research Center Activity Report 2019-2020*. State Meteorological Agency (AEMET), Madrid, Spain and World Meteorological Organization, Geneva, Switzerland <https://doi.org/10.31978/666-22-014-0> NIPO: 666-22-014-0, WMO/GAW Report No. 276.
- Dominguez-Rodriguez, A., Baez-Ferrer, N., Rodríguez, S., Avanzas, P., Abreu-Gonzalez, P., Terradellas, E., Cuevas, E., Basart, S., Werner, E., 2020. Saharan dust events in the Dust Belt - Canary Islands- and the observed association with in-hospital mortality of patients with heart failure. *J. Clin. Med.* 9, 376. <https://doi.org/10.3390/jcm9020376>.
- EC, 2008. Directive 2008/50/EC of the European Parliament and of the Council of 21 May 2008 on ambient air quality and cleaner air for Europe. *Off. J. Eur. Union L* 52, 11.6.2008, pp. 1–44.
- EEA, 2021. European Union emission inventory report 1990-2019. EEA Report No 05/2021 <https://doi.org/10.2800/701303>.
- Filonchik, M., Peterson, M.P., Gusev, A., Hu, F., Yan, H., Zhou, L., 2022. Measuring air pollution from the 2021 Canary Islands volcanic eruption. *Sci. Total Environ.* 849, 157827. <https://doi.org/10.1016/j.scitotenv.2022.157827>.
- Freire, S., Florczyk, A.J., Pesaresi, M., Sliuzas, R., 2019. An improved global analysis of population distribution in proximity to active volcanoes, 1975–2015. *ISPRS Int. J. Geo Inf.* 8, 341. <https://doi.org/10.3390/ijgi8080341>.
- Freudenthaler, V., Esselborn, M., Wiegner, M., Heese, B., Tesche, M., Ansmann, A., Müller, D., Althausen, D., Wirth, M., Fix, A., Ehret, G., Knippertz, P., Toledano, C., Gasteiger, J., Garhammer, M., Seefeldner, M., 2009. Depolarization ratio profiling at several wavelengths in pure saharan dust during SAMUM2006. *Tellus B Chem. Phys. Meteorol.* 61, 165–179. <https://doi.org/10.1111/j.1600-0889.2008.00396.x>.
- García, O., Suárez, D., Cuevas, E., Ramos, R., Barreto, A., et al., 2022. La erupción volcánica de La Palma y el papel de la Agencia Estatal de Meteorología. *Revista Tiempo Y Clima. 5* .. <https://pub.ame-web.org/index.php/TyC/article/view/2516>.
- Gauthier, P.J., Sigmarsson, O., Gouhier, M., Haddadi, B., Mouné, S., 2016. Elevated gas flux and trace metal degassing from the 2014–2015 fissure eruption at the Bárðarbunga volcanic system, Iceland. *Journal of Geophysical Research: Solid Earth* 121, 1610–1630. <https://doi.org/10.1002/2015JB012111>.
- Gettelman, A., Schmidt, A., Egill Kristjánsson, J., 2015. Icelandic volcanic emissions and climate. *Nat. Geosci.* 8. <https://doi.org/10.1038/ngeo2376> 243–243.
- Gíslason, S., Stefánssdóttir, G., Pfeffer, M., Barsotti, S., Jóhannsson, T., Galeczka, I., Bali, E., Sigmarsson, O., Stefánsson, A., Keller, N., Sigurdsson, Bergsson, B., Galle, B., Jacobo, V., Arellano, S., Aiuppa, A., Jónsdóttir, E., Eiríksdóttir, E., Jakobsson, S., Guðfinnsson, G., Halldórsson, S., Gunnarsson, H., Haddadi, B., Jónsdóttir, I., Thordarson, T., Ríisshuus, M., Högnadóttir, T., Dürrig, T., Pedersen, G., Höskuldsson, Gudmundsson, M., 2015. Environmental pressure from the 2014–15 eruption of Bárðarbunga volcano, Iceland. *Geochemical Perspectives Letters*, 84–93. <https://doi.org/10.7185/geochemlet.1509>.
- González, Y., 2012. Levels and origin of reactive gases and their relationship with aerosols in the proximity of the emission sources and in the free troposphere at Tenerife PhD Thesis. *Technical Note N° 12, AEMET, NIPO 281-12-016-1*.
- González, P.J., 2022. Volcano-tectonic control of cumbre vieja. *Science* 375, 1348–1349. <https://doi.org/10.1126/science.abn5148>.
- Hernández-Pacheco, A., Valls, M.C., 1982. The historic eruptions of La Palma Island (Canarias). *Arquipelago. Série Ciências da Naturezas* 3, pp. 83–94.
- Hersbach, H., Bell, B., Berrisford, P., Hirahara, S., Horányi, A., Muñoz-Sabater, J., Nicolas, J., Peubey, C., Radu, R., Schepers, D., Simmons, A., Soci, C., Abdalla, S., Abellan, X., Balsamo, G., Bechtold, P., Biavati, G., Bidlot, J., Bonavita, M., Chiara, G.D., Dahlgren, P., Dee, D., Diamantakis, M., Dragani, R., Flemming, J., Forbes, R., Fuentes, M., Geer,
- A., Haimberger, L., Healy, S., Hogan, R.J., Hólm, E., Janisková, M., Keeley, S., Laloyaux, P., Lopez, P., Lupu, C., Radnoti, G., Rosnay, P.D., Rozum, I., Vamborg, F., Villaume, S., Thépaut, J.N., 2020. The ERA5 global reanalysis. *Quarterly Journal of the Royal Meteorological Society* 146, 1999–2049. <https://doi.org/10.1002/qj.3803>.
- Ilyinskaya, E., Schmidt, A., Mather, T.A., Pope, F.D., Witham, C., Baxter, P., Jóhannsson, T., Pfeffer, M., Barsotti, S., Singh, A., Sanderson, P., Bergsson, B., McCormick Kilbride, B., Donovan, A., Peters, N., Oppenheimer, C., Edmonds, M., 2017. Understanding the environmental impacts of large fissure eruptions: aerosol and gas emissions from the 2014–2015 holuhraun eruption (Iceland). *Earth Planet. Sci. Lett.* 472, 309–322. <https://doi.org/10.1016/j.epsl.2017.05.025>.
- ISTAC, 2021. Official Population Figures Referring to Revision of Municipal Register 1 January, 2021. Canary Islands Statistic Institute, Spain. <http://www.gobiernodecanarias.org/istac/estadisticas/>.
- Landrigan, P.J., Fuller, R., Acosta, N.J.R., Adeyi, O., Arnold, R., Basu, N.N., Baldé, A.B., Bertollini, R., Bose-O'Reilly, S., Boufford, J.L., et al., 2018. The lancet commission on pollution and health. *Lancet* 391, 462–512. [https://doi.org/10.1016/S0140-6736\(17\)32345-0](https://doi.org/10.1016/S0140-6736(17)32345-0).
- Langmann, B., Folch, A., Hensch, M., Matthias, V., 2012. Volcanic ash over Europe during the eruption of Eyjafjallajökull on Iceland, April–May 2010. *Atmos. Environ.* 48, 1–8. <https://doi.org/10.1016/j.atmosenv.2011.03.054>.
- Longo, B.M., 2013. Adverse health effects associated with increased activity at Kilauea volcano: a repeated population-based survey. *ISRN Public Health* 2013, 475962. <https://doi.org/10.1155/2013/475962>.
- Longpré, M.A., 2021. Reactivation of cumbre Vieja volcano. *Science* 374, 1197–1198. <https://doi.org/10.1126/science.abm9423>.
- Longpré, M.A., Felpeo, A., 2021. Historical volcanism in the Canary Islands; part 1: a review of precursory and eruptive activity, eruption parameter estimates, and implications for hazard assessment. *J. Volcanol. Geotherm. Res.* 419, 107363. <https://doi.org/10.1016/j.jvolgeores.2021.107363>.
- Lopez, C., Blanco, M.J., Team, I.G.N., 2022. Instituto Geográfico Nacional Volcano Monitoring of the 2021 La Palma eruption (Canary Islands, Spain). EGU General Assembly 2022, Vienna, Austria, 23–27 May 2022, EGU22-11549. <https://doi.org/10.5194/egusphere-egu22-11549>.
- Milford, C., Cuevas, E., Marrero, C.L., Bustos, J.J., Gallo, V., Rodríguez, S., Romero-Campos, P.M., Torres, C., 2020. Impacts of desert dust outbreaks on air quality in urban areas. *Atmosphere* 11, 23. <https://doi.org/10.3390/atmos11010023>.
- Miteco, 2021. Episodios naturales de Partículas 2020 ministerio Para la Transición Ecológica y el reto Demográfico, Madrid, Spain. available at: [https://www.miteco.gob.es/es/calidad-y-evaluacion-ambiental/temas/atmosfera-y-calidad-del-aire/episodiosnaturales2020\\_tcm30-529865.pdf](https://www.miteco.gob.es/es/calidad-y-evaluacion-ambiental/temas/atmosfera-y-calidad-del-aire/episodiosnaturales2020_tcm30-529865.pdf).
- MITECO, 2022. *Inventario Nacional de Emisiones a la Atmósfera. Emisiones de Contaminantes Atmosféricos. Serie 1990-2020. Informe Resumen. Ministerio para la Transición Ecológica y el Reto Demográfico, Madrid, Spain.*
- Newnham, R.M., Dirks, K.N., Samaranyake, D., 2010. An investigation into long-distance health impacts of the 1996 eruption of mt ruapehu, New Zealand. *Atmos. Environ.* 44, 1568–1578. <https://doi.org/10.1016/j.atmosenv.2009.12.040>.
- Nogales, M., Guerrero-Campos, M., Boulesteix, T., Taquet, N., Beierkuhnlein, C., Campion, R., Fajardo, S., Zurita, N., Arechavaleta, M., García, R., Weiser, F., Medina, F.M., 2022. The fate of terrestrial biodiversity during an oceanic island volcanic eruption. *Sci. Rep.* 12, 19344. <https://doi.org/10.1038/s41598-022-22863-0>.
- Orellano, P., Reynoso, J., Quaranta, N., Bardach, A., Ciapponi, A., 2020. Short-term exposure to particulate matter (PM10 and PM2.5), nitrogen dioxide (NO2), and ozone (O3) and all-cause and cause-specific mortality: systematic review and meta-analysis. *Environ. Int.* 142, 105876. <https://doi.org/10.1016/j.envint.2020.105876>.
- Orellano, P., Reynoso, J., Quaranta, N., 2021. Short-term exposure to Sulphur dioxide (SO2) and all-cause and respiratory mortality: a systematic review and meta-analysis. *Environ. Int.* 150, 106434. <https://doi.org/10.1016/j.envint.2021.106434>.
- PEVOLCA, 2021. Scientific Committee Report 25/12/2021: Actualización de la actividad volcánica en Cumbre Vieja (La Palma). <https://info.igme.es/eventos/Erupcion-volcanica-la-palma/pevolca>.
- Pisani, G., Boselli, A., Coltelli, M., Leto, G., Pica, G., Scollo, S., Spinelli, N., Wang, X., 2012. Lidar depolarization measurement of fresh volcanic ash from mt. Etna Italy. *Atmospheric Environment* 62, 34–40. <https://doi.org/10.1016/j.atmosenv.2012.08.015>.
- Prospero, J.M., Mayol-Bracero, O.L., 2013. Understanding the transport and impact of african dust on the Caribbean Basin. *Bull. Am. Meteorol. Soc.* 94, 1329–1337. <https://doi.org/10.1175/BAMS-D-12-00142.1>.
- Prospero, J.M., Delany, A.C., Delany, A.C., Carlson, T.N., 2021. The discovery of african dust transport to the Western hemisphere and the saharan air layer: a history. *Bull. Am. Meteorol. Soc.* -1, 1–53. <https://doi.org/10.1175/BAMS-D-19-0309.1>.
- Rodríguez, S., Calzola, G., Chiari, M., Nava, S., García, M.I., López-Solano, J., Marrero, C., López-Darías, J., Cuevas, E., Alonso-Pérez, S., Prats, N., Amato, F., Lucarelli, F., Querol, X., 2020. Rapid changes of dust geochemistry in the saharan air layer linked to sources and meteorology. *Atmos. Environ.* 223, 117186. <https://doi.org/10.1016/j.atmosenv.2019.117186>.
- Romahn, F., Pedergnana, M., Loyola, D., Apituley, A., Sneep, M., Veeffkind, J.P., 2022. S5P/TROPOMI L2 Product User Manual Sulphur Dioxide SO2 - S5P-L2-DLR-PUM-400E. 02.04.00. Available at.
- Román, A., Tovar-Sánchez, A., Roque-Atienza, D., Huertas, I., Caballero, I., Fraile-Nuez, E., Navarro, G., 2022. Unmanned aerial vehicles (UAVs) as a tool for hazard assessment: the 2021 eruption of cumbre Vieja volcano, La Palma Island (Spain). *Sci. Total Environ.* 843, 157092. <https://doi.org/10.1016/j.scitotenv.2022.157092>.
- Ruano-Ravina, A., Acosta, O., Díaz Pérez, D., Casanova, C., Velasco, V., Peces-Barba, G., Barreiro, E., Cañas, A., Castaño, A., Cruz Carmona, M.J., Diego, C., García-Aymerich, J., Martínez, C., Molina-Molina, M., Muñoz, X., Sánchez-Íñigo, F.J., Candal-Pedreira, C., 2023. A longitudinal and multidisciplinary epidemiological study to analyze the effect of the volcanic eruption of tajogaite volcano (La Palma, Canary Islands) The ASHES study protocol. *Environ. Res.* 216, 114486. <https://doi.org/10.1016/j.envres.2022.114486>.

- Schäfer, K., Thomas, W., Peters, A., Ries, L., Obleitner, F., Schnelle-Kreis, J., Birmili, W., Diemer, J., Fricke, W., Junkermann, W., Pitz, M., Emeis, S., Forkel, R., Suppan, P., Flentje, H., Gilge, S., Wichmann, H.E., Meinhardt, F., Zimmermann, R., Weinhold, K., Soentgen, J., Münkler, C., Freuer, C., Cyrys, J., 2011. Influences of the 2010 Eyjafjallajökull volcanic plume on air quality in the northern alpine region. *Atmos. Chem. Phys.* 11, 8555–8575. <https://doi.org/10.5194/acp-11-8555-2011>.
- Schmidt, A., Leadbetter, S., Theys, N., Carboni, E., Witham, C.S., Stevenson, J.A., Birch, C.E., Thordarson, T., Turnock, S., Barsotti, S., Delaney, L., Feng, W., Grainger, R.G., Hort, M.C., Höskuldsson, I., Ilyinskaya, E., Jóhannsson, T., Kenny, P., Mather, T.A., Richards, N.A.D., Shepherd, J., 2015. Satellite detection, long-range transport, and air quality impacts of volcanic sulfur dioxide from the 2014–2015 flood lava eruption at Bárðarbunga (Iceland). *J. Geophys. Res.-Atmos.* 120, 9739–9757. <https://doi.org/10.1002/2015JD023638>.
- Scollo, S., Boselli, A., Coltelli, M., Leto, G., Pisani, G., Spinelli, N., Wang, X., 2012. Monitoring Etna volcanic plumes using a scanning LiDAR. *Bull. Volcanol.* 74, 2383–2395. <https://doi.org/10.1007/s00445-012-0669-y>.
- Searl, A., Nicholl, A., Baxter, P., 2002. Assessment of the exposure of islanders to ash from the Soufrière Hills volcano, Montserrat, British West Indies. *Occup. Environ. Med.* 59, 523–531. <https://doi.org/10.1136/oem.59.8.523>.
- Sicard, M., Córdoba-Jabonero, C., Barreto, A., Welton, E.J., Gil-Díaz, C., Carvajal-Pérez, C.V., Comerón, A., García, O., García, R., López-Cayuela, M., Muñoz-Porcar, C., Prats, N., Ramos, R., Rodríguez-Gómez, C., Toledano, C., Torres, C., 2022. Volcanic eruption of Cumbre Vieja, La Palma, Spain: a first insight to the particulate matter injected in the troposphere. *Remote Sens.* 14, 2470. <https://doi.org/10.3390/rs14102470>.
- Stewart, C., Damby, D.E., Horwell, C.J., Elias, T., Ilyinskaya, E., Tomašek, I., Longo, B.M., Schmidt, A., Carlsen, H.K., Mason, E., Baxter, P.J., Cronin, S., Witham, C., 2021. Volcanic air pollution and human health: recent advances and future directions. *Bull. Volcanol.* 84, 11. <https://doi.org/10.1007/s00445-021-01513-9>.
- Stohl, A., Seibert, P., 1998. Accuracy of trajectories as determined from the conservation of meteorological tracers. *Q. J. R. Meteorol. Soc.* 124, 1465–1484. <https://doi.org/10.1002/qj.49712454907>.
- Stohl, A., Wotawa, G., Seibert, P., Kromp-Kolb, H., 1995. Interpolation errors in wind fields as a function of spatial and temporal resolution and their impact on different types of kinematic trajectories. *J. Appl. Meteorol. Climatol.* 34, 2149–2165. [https://doi.org/10.1175/1520-0450\(1995\)034<2149:IEIWFA>2.0.CO;2](https://doi.org/10.1175/1520-0450(1995)034<2149:IEIWFA>2.0.CO;2).
- Tang, Y., Tong, D.Q., Yang, K., Lee, P., Baker, B., Crawford, A., Luke, W., Stein, A., Campbell, P.C., Ring, A., Flynn, J., Wang, Y., McQueen, J., Pan, L., Huang, J., Stajner, I., 2020. Air quality impacts of the 2018 mt. Kilauea Volcano eruption in Hawaii: aregional chemical transport model study with satellite-constrained emissions. *Atmos. Environ.* 237, 117648. <https://doi.org/10.1016/j.atmosenv.2020.117648>.
- Theys, N., De Smedt, I., Yu, H., Danckaert, T., van Gent, J., Hörmann, C., Wagner, T., Hedelt, P., Bauer, H., Romahn, F., Pedernana, M., Loyola, D., Van Roozendael, M., 2017. Sulfur dioxide retrievals from TROPOMI onboard Sentinel-5 precursor: algorithm theoretical basis. *Atmos. Meas. Tech.* 10, 119–153. <https://doi.org/10.5194/amt-10-119-2017>.
- Thomas, H.E., Prata, A.J., 2011. Sulphur dioxide as a volcanic ash proxy during the April–May 2010 eruption of Eyjafjallajökull volcano, Iceland. *Atmos. Chem. Phys.* 11, 6871–6880. <https://doi.org/10.5194/acp-11-6871-2011>.
- Thomas, M.A., Brännström, N., Persson, C., Grahm, H., von Schoenberg, P., Robertson, L., 2017. Surface air quality implications of volcanic injection heights. *Atmos. Environ.* 166, 510–518. <https://doi.org/10.1016/j.atmosenv.2017.07.045>.
- Torres-González, P., Luengo-Oroz, N., Lamolda, H., D'Alessandro, W., Albert, H., Iribarren, I., Moure-García, D., Soler, V., 2020. Unrest signals after 46 years of quiescence at cumbre vieja, La Palma, Canary Islands. *J. Volcanol. Geotherm. Res.* 392, 106757. <https://doi.org/10.1016/j.jvolgeores.2019.106757>.
- Trejos, E.M., Silva, L.F.O., Hower, J.C., Flores, E.M.M., González, C.M., Pachón, J.E., Aristizábal, B.H., 2021. Volcanic emissions and atmospheric pollution: a study of nanoparticles. *Geosci. Front.* 12, 746–755. <https://doi.org/10.1016/j.gsf.2020.08.013>.
- Tsamalis, C., Chédin, A., Pelon, J., Capelle, V., 2013. The seasonal vertical distribution of the saharan air layer and its modulation by the wind. *Atmos. Chem. Phys.* 13, 11235–11257. <https://doi.org/10.5194/acp-13-11235-2013>.
- Tu, F.H., Thornton, D.C., Bandy, A.R., Carmichael, G.R., Tang, Y., Thornhill, K.L., Sachse, G.W., Blake, D.R., 2004. Long-range transport of sulfur dioxide in the Central Pacific. *Journal of Geophysical Research: Atmospheres* 109. <https://doi.org/10.1029/2003JD004309>.
- Twigg, M.M., Ilyinskaya, E., Beccaceci, S., Green, D.C., Jones, M.R., Langford, B., Leeson, S.R., Lingard, J.J.N., Pereira, G.M., Carter, H., Poskitt, J., Richter, A., Ritchie, S., Simmons, I., Smith, R.L., Tang, Y.S., Van Dijk, N., Vincent, K., Nemitz, E., Vieno, M., Braban, C.F., 2016. Impacts of the 2014–2015 hólhraun eruption on the UK atmosphere. *Atmos. Chem. Phys.* 16, 11415–11431. <https://doi.org/10.5194/acp-16-11415-2016>.
- Valade, S., Ley, A., Massimetti, F., D'Hondt, O., Laiolo, M., Coppola, D., Loibl, D., Hellwich, O., Walter, T.R., 2019. Towards global volcano monitoring using multisensor sentinel missions and artificial intelligence: the MOUNTS monitoring system. *Remote Sensing* 11. <https://doi.org/10.3390/rs11131528>.
- Viana, M., Querol, X., Alastuey, A., Cuevas, E., Rodriguez, S., 2002. Influence of african dust on the levels of atmospheric particulates in the Canary Islands air quality network. *Atmos. Environ.* 36, 5861–5875. [https://doi.org/10.1016/S1352-2310\(02\)00463-6](https://doi.org/10.1016/S1352-2310(02)00463-6).
- Weiser, F., Baumann, E., Jentsch, A., Medina, F.M., Lu, M., Nogales, M., Beierkuhnlein, C., 2022. Impact of volcanic sulfur emissions on the pine forest of La Palma Spain. *Forests* 13, 299. <https://doi.org/10.3390/f13020299>.
- Welton, E.J., Campbell, J.R., 2002. Micropulse lidar signals: uncertainty analysis. *J. Atmos. Ocean. Technol.* 19, 2089–2094. [https://doi.org/10.1175/1520-0426\(2002\)019<2089:MLSUA>2.0.CO;2](https://doi.org/10.1175/1520-0426(2002)019<2089:MLSUA>2.0.CO;2).
- Whitty, R.C.W., Ilyinskaya, E., Mason, E., Wieser, P.E., Liu, E.J., Schmidt, A., Roberts, T., Pfeffer, M.A., Brooks, B., Mather, T.A., Edmonds, M., Elias, T., Schneider, D.J., Oppenheimer, C., Dybwad, A., Nadeau, P.A., Kern, C., 2020. Spatial and temporal variations in SO<sub>2</sub> and PM<sub>2.5</sub> levels around Kilauea volcano, Hawaii during 2007–2018. *Frontiers Earth Sci.* 8. <https://doi.org/10.3389/feart.2020.00036>.
- WHO, 2006. *WHO Air Quality Guidelines: Global Update 2005 - Particulate Matter, Ozone, Nitrogen dioxide and Sulfur Dioxide*. World Health Organization, Regional Office for Europe, Copenhagen.
- WHO, 2013. *Review of Evidence on Health Aspects of Air Pollution - REVIHAAP Project*. World Health Organization, Regional Office for Europe, Copenhagen.
- WHO, 2016. *Ambient air pollution: A global assessment of exposure and burden of disease*. World Health Organization, Geneva, Switzerland.
- WHO, 2018. *Air pollution and child health: Prescribing clean air*. World Health Organization, Geneva, Switzerland.
- WHO, 2021. *WHO air quality guidelines. Particulate matter (PM<sub>2.5</sub> and PM<sub>10</sub>), ozone, nitrogen dioxide and sulfur dioxide*. World Health Organization, Geneva.
- WMO, 2018. *Guide to Meteorological Instruments and Methods of Observation No. 8*.

## Glossary

- AOD: Aerosol Optical Depth  
 AEMET: State Meteorological Agency of Spain  
 AQG: Air Quality Guideline  
 AQMN: Air Quality Monitoring Network  
 CSIC: Spanish National Research Council  
 EC: European Commission  
 ECMWF: European Centre for Medium-Range Weather Forecasts  
 FLEXTRA: FLEXible TRAJectories model  
 FT: Free Troposphere  
 HARMONIE-AROME: (HirLam Aladin Regional/Meso-scale Operational NWP in Euromed)  
 IARC: Izaña Atmospheric Research Center  
 IZO: Izaña Observatory  
 MBL: Marine Boundary Layer  
 MODIS: Moderate Resolution Imaging Spectroradiometer  
 MOUNTS: Monitoring Unrest from Space  
 MPL: Micropulse Lidar  
 MPLNET: Micropulse Lidar Network  
 NRT: Near Real Time  
 NWP: Numerical Weather Prediction  
 OPS: Optical Particle Sizer  
 PDR: Particle Depolarization Ratio  
 PEVOLCA: Plan Especial de Protección Civil y Atención de Emergencias por Riesgo Volcánico en la Comunidad Autónoma de Canarias  
 PM<sub>10</sub>: PM with aerodynamic diameter < 10 µm  
 PM<sub>2.5</sub>: PM with aerodynamic diameter < 2.5 µm  
 S-5P: Sentinel-5 Precursor  
 SAL: Saharan Air Layer  
 SCO: Santa Cruz Observatory  
 TROPOMI: TROPospheric Monitoring Instrument  
 TWI: Trade Wind Inversion  
 UVU: Ultraviolet  
 VDR: Volume Depolarization Ratio  
 WHO: World Health Organisation  
 WMO: World Meteorological Organization